



Article

Dominant-Negative Attenuation of cAMP-Selective Phosphodiesterase PDE4D Action Affects Learning and Behavior

Graeme B. Bolger ^{1,2,*} , Lisa High Mitchell Smoot ³ and Thomas van Groen ⁴

¹ Department of Medicine and Department of Pharmacology, University of Alabama at Birmingham, Birmingham, AL 35294-3300, USA

² BZI Pharma LLC, 1500 1st Ave N., Unit 36, Birmingham, AL 35203-1872, USA

³ Department of Medicine, University of Alabama at Birmingham, Birmingham, AL 35294, USA; lsmoot@uab.edu

⁴ Department of Cell, Developmental and Integrative Biology, University of Alabama at Birmingham, Birmingham, AL 35294, USA; vangroen@uab.edu

* Correspondence: gbbolger@uab.edu

Received: 5 July 2020; Accepted: 6 August 2020; Published: 9 August 2020



Abstract: PDE4 cyclic nucleotide phosphodiesterases reduce 3', 5' cAMP levels in the CNS and thereby regulate PKA activity and the phosphorylation of CREB, fundamental to depression, cognition, and learning and memory. The PDE4 isoform PDE4D5 interacts with the signaling proteins β -arrestin2 and RACK1, regulators of β_2 -adrenergic and other signal transduction pathways. Mutations in *PDE4D* in humans predispose to acrodysostosis, associated with cognitive and behavioral deficits. To target PDE4D5, we developed mice that express a PDE4D5-D556A dominant-negative transgene in the brain. Male transgenic mice demonstrated significant deficits in hippocampus-dependent spatial learning, as assayed in the Morris water maze. In contrast, associative learning, as assayed in a fear conditioning assay, appeared to be unaffected. Male transgenic mice showed augmented activity in prolonged (2 h) open field testing, while female transgenic mice showed reduced activity in the same assay. Transgenic mice showed no demonstrable abnormalities in prepulse inhibition. There was also no detectable difference in anxiety-like behavior, as measured in the elevated plus-maze. These data support the use of a dominant-negative approach to the study of PDE4D5 function in the CNS and specifically in learning and memory.

Keywords: learning; memory; PKA; CREB; PDE4; PDE4D5; RACK1; β -arrestin2; acrodysostosis

1. Introduction

Highly selective inhibitors of the PDE4, 3', 5'-cAMP-specific phosphodiesterases have proven cognition-enhancing and antidepressant properties in humans [1–12] and rodents [13–48]. PDE4-selective inhibitors are exploited therapeutically for their anti-inflammatory, immunomodulatory and smooth-muscle relaxant activities (for reviews, see [49–51]). At present, three PDE4-selective inhibitors, roflumilast, apremilast, and crisaborole, are in clinical use for a wide range of respiratory and inflammatory disorders [52–54]. A PDE3/4-selective inhibitor, ensifentrine (RPL554), is in mid-stage clinical trials for chronic obstructive pulmonary disease [55,56]. A number of PDE4-selective inhibitors are under development specifically for CNS indications, including depression and as enhancers of learning and memory [9–12,45–48,57–63].

PDE4-selective inhibitors inhibit the enzymatic hydrolysis of cAMP and thereby increase its levels in cells. One of their major effects is to activate cAMP-dependent protein kinase (PKA) and thereby stimulate the phosphorylation of its physiological substrates, including the cyclic nucleotide response

element-binding protein (CREB). Activation of CREB is essential for numerous CNS functions, notably learning and memory (for reviews, see [64–66]) and depression [67]. Additional targets of cAMP in the CNS include the exchange protein directly activated by cAMP (EPAC), cyclic-nucleotide-gated ion channels, and popeye-domain-containing proteins [68–71]. There are over 20 PDE4 isoforms, which are encoded by 4 genes in mammals (in humans, *PDE4A*, *PDE4B*, *PDE4C*, and *PDE4D*), each of which produces a range of isoforms by the use of alternative promoters and alternative mRNA splicing specific for each isoform [72,73]. Each isoform has a distinct tissue-specific pattern of mRNA and protein expression, including significant regional expression differences in the CNS, suggesting that each has a distinct biological function [74–84]. All PDE4-selective inhibitors that have been synthesized to date interact with the catalytic sites of the PDE4 enzymes and therefore act, to a considerable extent, as competitive inhibitors of cAMP hydrolysis [49,85–87]. The catalytic sites of the various PDE4 isoforms are extremely similar, posing a challenge to the development of truly isoform-selective PDE4 inhibitors [86].

One of the best-studied PDE4 isoforms is PDE4D5, which is 1 of 11 isoforms encoded by the mouse *Pde4d* gene and which is highly conserved among mammals (Figure 1a,b, [88]). Each PDE4D isoform is expressed off a different promoter and has a unique expression pattern in the CNS [74,76–78,82,89–95]. For example, in situ studies using riboprobes have shown that each of the PDE4D1, -2, -3, -4, and -5 mRNAs (Figure 1a) have a distinct distribution pattern in the brain, correlating in some cases with specific brain pathways. PDE4D2 mRNA transcripts are expressed in the dorsal and median raphe nuclei, probably located in serotonergic cells. PDE4D1 and PDE4D2 mRNA splice forms are both expressed in the area postrema, whereas the cellular distribution of PDE4D4 and PDE4D5 shows a complementary pattern [77]. Other studies have shown that PDE4D isoforms are localized to neurons in the nodose ganglion and in many structures of the medulla, including neurons of the nucleus tractus solitarius and locus coeruleus [89]. Collectively, these data suggest that each isoform has a unique partially non-overlapping role; however, this needs to be confirmed by functional studies of each of these isoforms.

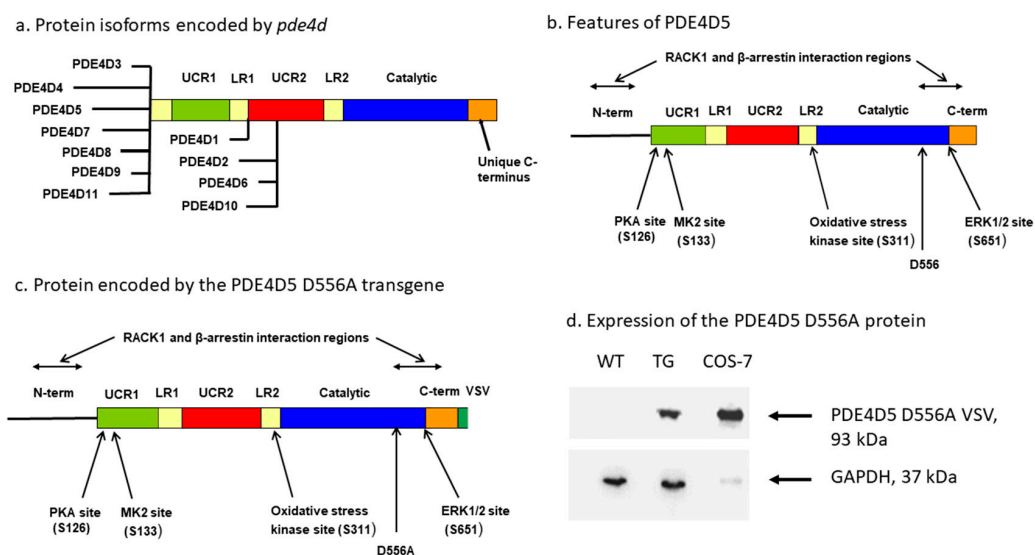


Figure 1. (a) Proteins encoded by the human *PDE4D* gene [73,88,96–100]. The long isoforms PDE4D3, PDE4D4, PDE4D5, PDE4D7, PDE4D8, PDE4D9, and PDE4D11 all contain UCR1, UCR2, and catalytic domains, separated by the unstructured LR1 and LR2 regions. The short isoform PDE4D1 contains the catalytic domain and UCR2, while the super-short PDE4D2, PDE4D6, and PDE4D10 isoforms contain the catalytic region and a portion of UCR2. UCR1 and UCR2 mediate dimerization of the long PDE4D isoforms. Each isoform also contains isoform-specific unique regions at its amino-terminus (heavy black lines). The carboxyl-terminal region (C-terminus) is also shown, which is common to all PDE4D isoforms

but which differs from the carboxyl-terminal regions of PDE4A, PDE4B, and PDE4C isoforms. (b) Features of PDE4D5. The 88-amino-acid unique amino-terminal region (N-term) of PDE4D5 is indicated (heavy black line), along with the C-terminus (C-term) and regions required for its interaction with RACK1 and β -arrestin2. The PKA site and MK2 site are also shown, both located within UCR1, the oxidative stress kinase site located within LR2, the ERK1/2 site located in the catalytic region, and D556, the amino acid mutated in this study. (c) Protein encoded by the PDE4D5 D556A transgene. Features as in b, but with the D556A mutation and the VSV epitope at the carboxyl-terminus. (d) Immunoblotting of whole-brain extracts (10 μ g protein/lane) from wild-type (WT) and transgenic (TG) mice. Extract from COS-7 cells (1 μ g protein/lane) transfected to express PDE4D5-D556A-VSV was run as a size standard (COS-7). Immunoblotting with anti-VSV detected a 93-kDa protein (top). Immunoblotting with anti-GAPDH, serving as a loading control, detected a 37-kDa protein (bottom).

PDE4D5 interacts selectively and at high avidity with several signaling proteins, most notably RACK1 [101–107], β -arrestin2 [103,108–114], and also several elements of MAPK signaling, notably ERK1/2 [115–117] and MK2 [118,119]. RACK1 and β -arrestin2 both interact much more avidly with PDE4D5 than with any other PDE4D isoform [101,110]. PDE4D5 is also the target of several additional kinases, most notably PKA [120–123] and oxidative-stress kinases [124] (Figure 1b). Collectively, the phosphorylation state of PDE4D5 that is produced by the cumulative effects of these kinases alters the enzymatic activity of the kinase (velocity), its affinity for its substrate, cAMP, and various PDE4-selective inhibitors, its interactions with its protein partners, and its intracellular localization.

To expand our knowledge of the functional roles of various PDE4 isoforms in the CNS, and as a stimulus to drug development, we adopted a dominant-negative approach. We and our collaborators utilized this approach initially to study the functions of PDE4D5 in cell-based assays [103,108,109,111]. This dominant-negative mutation is in a single amino acid (D556A in PDE4D5, conserved in all PDE4 isoforms) in a specific metal-ion-binding site in the catalytic region of PDE4D5 that has been identified by X-ray crystallographic analysis as being essential for catalysis [125,126]. Mutation of this amino acid to alanine dramatically reduces (<99% reduction) the enzyme's catalytic activity [103,108,109]. When PDE4D5-D556A is overexpressed in cells, this mutant does not detectably change total PDE4D enzymatic activity but produces an equilibrium displacement of endogenous PDE4D5 from its protein partners, most notably RACK1 and β -arrestin2, or affects the ability of the PDE4 isoform to homodimerize [107,127–131], and therefore disrupts the cellular functions of PDE4D5 in a dominant-negative fashion [103,108,109,111,132]. The cellular effects of PDE4D5-D556A have been studied most extensively in cells exhibiting the action of the β_2 -adrenergic receptor (β_2 AR; [103,108,109,111]). In these experiments, PDE4D5-D556A-mediated displacement of β -arrestin2 from wild-type PDE4D5 prevented β -arrestin2 from recruiting wild-type PDE4D5 to the β_2 AR, thereby blocking cAMP-mediated downregulation of the β_2 AR by PKA [108,109]. This blocked the β -arrestin2-mediated switch of the β_2 AR from G_s to G_i and thereby activated the ERK1/2 kinase pathway [103,109,111].

Recently, we extended our dominant-negative approach to the functional study of PDE4 isoforms in the CNS [133]. Our first study focused on an important PDE4B isoform, specifically PDE4B1. For this work, we developed mice that expressed a dominant-negative mutant, PDE4B1-D564A (corresponding to the D556A mutation in PDE4D5), in the murine forebrain and hippocampus. This PDE4B1-D564A-encoding transgene markedly affected behavior, as measured in open-field testing, and produced significant alterations in the phosphorylation of critical substrates and in hippocampal synaptic plasticity [133]. This and similar dominant-negative strategies [134–136] expand on other genetic approaches that have been used to study PDE4 function in the CNS, such as gene knockouts [27,137–143] and lentiviral siRNA [142,144–147], but are potentially more isoform-selective.

Cell-based assays and animal studies have demonstrated a plausible functional role for PDE4D5 in numerous cellular functions, including β_2 -adrenergic signaling [108,109,111,112,148,149], airway smooth muscle function [150–152], cell spreading and motility in culture [153], and immunity/inflammation [154]. However, given the significant CNS actions of PDE4-selective inhibitors,

we were particularly interested in determining the precise function(s) of PDE4D5 in the CNS. Therefore, we aimed to determine whether the PDE4D5-D556A mutant, when expressed as a transgene in the brain, affected behavior. Given the potential CNS uses of PDE4-selective inhibitors, and the potential correlations between depressive disorders and cognitive and neurophysiological symptoms [58,59], we were particularly interested in testing the effect of PDE4D5-D556A on cognition, activity, learning and memory, and on measures of anxiety or depression.

2. Results

2.1. Mice Expressing a PDE4D5-D556A Transgene in the CNS

Our transgenic mice expressed PDE4D5-D556A (Figure 1c) under the control of the α -calmodulin kinase II (α CaMKII) promoter [155–157]. They were generated specifically for this paper using techniques we described previously [133]. During breeding, the PDE4D5-D556A transgene was inherited at the expected Mendelian frequency, showing that the transgene did not produce toxicity or affect fetal viability. PDE4D5-D556A transgenic mice were grossly indistinguishable from wild-type littermates and commercially available C57BL/6J mice. They grew at a normal rate and attained a normal adult size. Immunoblotting detected the expression of PDE4D5-D556A in transgenic but not wild-type, mice (Figure 1d).

2.2. Basic Neurologic Functions in PDE4D5-D556A Transgenic Mice

We assessed basic aspects of PDE4D5-D556A mice using the SHIRPA protocol [158,159]. This protocol tested measurements of physical characteristics, sensorimotor reflexes, general behavior, motor responses, grip strength, and included the Rotarod test and the wire suspension test, as described [133]. Wild-type and PDE4D5-D556A transgenic mice littermates were indistinguishable in these assays.

2.3. Effects of the PDE4D5-D556A Transgene on Activity in a Novel Open Field

We noted no significant difference between wild-type and PDE4D5-D556A transgenic littermates after only 10 min of observation in an open field. However, over a 2-h observation period, we noted statistically significant differences in both males and females (Figure 2). PDE4D5-D556A transgenic males, compared to wild-type males, had increased total activity (total ambulatory distance, Figure 2a, TG vs. WT, $p = 0.008$, $F(1,7) = 13.29$; for all male comparisons, $n = 5$ WT, $n = 5$ TG), and total ambulatory time (Figure 2b, $p = 0.09$, $F(1,7) = 3.83$). Females showed the opposite effect (Figure 2c,d, total ambulatory distance, TG vs. WT, $p = 0.007$, $F(1,7) = 13.87$; total ambulatory time, $p = 0.007$, $F(1,7) = 13.52$; for all female comparisons, $n = 5$ WT, $n = 5$ TG). Ambulatory distance for the total 2-h period was 2380 ± 54 cm for transgenic males compared to 1992 ± 208 cm for wild-type males, and 1928 ± 293 cm for transgenic females compared to 2342 ± 403 cm for wild-type females (means \pm SEM). We saw no detectable effect on vertical time (data for males, Figure 2e, TG vs. WT, $p = 0.5$, $F(1,7) = 0.48$, and for females, Figure 2f, TG vs. WT, $p = 0.9$, $F(1,7) = 0.28$). The effect of the PDE4D5-D556A transgene in males appeared robust, in that transgenic males also showed increased activity in the periphery of the field (ambulatory distance in the periphery, Figure 2g, TG vs. WT, $p = 0.028$, $F(1,7) = 7.60$) although ambulatory time in the periphery was not different (Figure 2h, TG vs. WT, $p = 0.26$, $F(1,7) = 1.50$). The reverse effect seen in females also appeared to be robust (Figure 2i,j, ambulatory distance in periphery, TG vs. WT, $p = 0.017$, $F(1,7) = 9.68$, and ambulatory time in periphery, $p = 0.028$, $F(1,7) = 7.63$).

As is typical for this assay, activity declined over the 2-h time course of the experiment. This effect was similar between PDE4D5-D556A transgenic and wild-type males (first vs. second hour, TG vs. WT: total ambulatory distance, $p = 0.8$, $F(1,7) = 0.054$; total ambulatory time, $p = 0.02$, $F(1,7) = 8.50$; distance in periphery, $p = 0.7$, $F(1,7) = 0.14$; time in periphery, $p = 0.7$, $F(1,7) = 0.13$). It was also similar between PDE4D5-D556A transgenic and wild-type females (first vs. second hour, TG vs. WT: total ambulatory distance, $p = 0.5$, $F(1,7) = 0.41$; total ambulatory time, $p = 0.4$, $F(1,7) = 0.69$; distance in periphery, $p = 0.3$, $F(1,7) = 1.13$; time in periphery, $p = 0.3$, $F(1,7) = 1.28$).

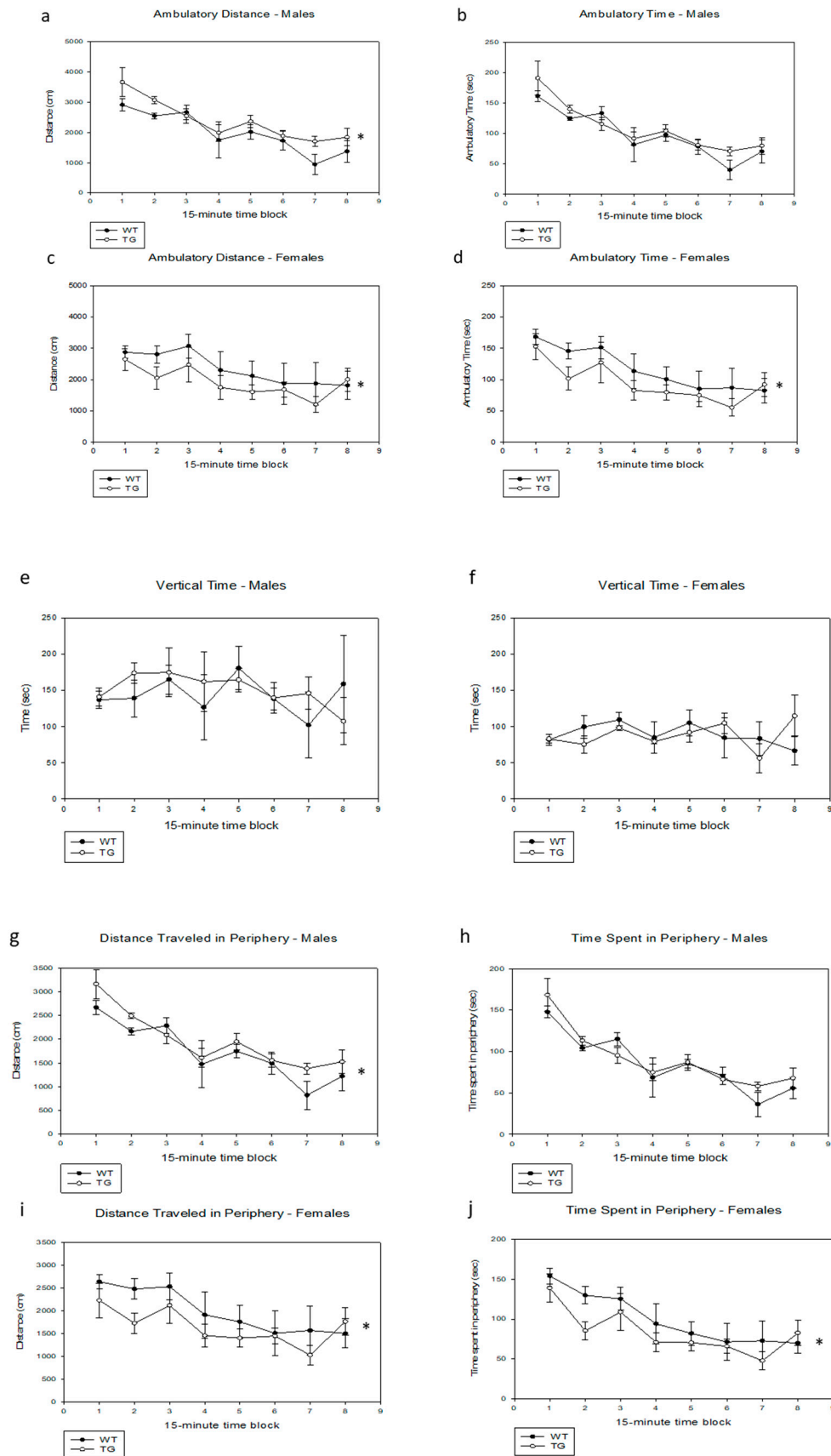


Figure 2. Activity of PDE4D5-D556A transgenic mice in an open field. Testing was performed for 2 h and activity analyzed for each 15-min block. Data are means \pm SE; asterisks (*) indicate data from the

transgenic mice that were statistically different over the 2-h testing period from that obtained from wild-type mice. (a) Ambulatory distance, males (b) Ambulatory time, males (c) Ambulatory distance, females (d) Ambulatory time, females (e) Vertical time, males (f) Vertical time, females (g) Distance traveled in periphery, males (h) Time spent in periphery, males (i) Distance traveled in periphery, females (j) Time spent in periphery, females.

2.4. Lack of Effect of the PDE4D5-D556A Transgene on Acoustic Startle and Prepulse Inhibition (PPI)

PDE4-selective inhibitors have been investigated as a potential therapy for schizophrenia and major affective disorders [28,83]. Of the various PDE4 isoforms, those encoded by *PDE4B* have been most closely associated with schizophrenia and major affective disorders and have been shown to interact directly with DISC1, a protein implicated in neurodevelopment, nuclear functions, and susceptibility to schizophrenia in humans [160–164]. Mice with mutations in *Disc1* have a diverse behavioral phenotype, including alterations in PPI [83,165,166]. However, in a recent study, we were unable to detect any effect of the PDE4B1-D564A transgene on PPI [133]. Given these considerations, we were motivated to determine any potential effect of the PDE4D5-D556A transgene on PPI (Figure 3a,b). We were unable to detect any difference in PPI in PDE4D5-D556A transgenic mice (Figure 3a; inhibition (%) at prepulses of 4, 8, and 16 dB above background, TG vs. WT, sexes pooled: $p = 0.64, 0.56$ and 0.26 , respectively, $F(1,18) = 0.22, 0.35$ and 1.34 , respectively; for males: $p = 0.18, 0.08$ and 0.016 , respectively, $F(1,8) = 2.16, 3.80, 9.26$, respectively; for females: $p = 0.55, 0.39, 0.63$, respectively, $F(1,8) = 0.38, 0.82$, and 0.26 , respectively). There was no detectable difference in the startle amplitude (Figure 3b; sexes pooled: $p = 0.52$, $F(1,18) = 0.43$; $n = 10$ WT, $n = 12$ TG; for males: $p = 0.12$, $F(1,8) = 2.99$; $n = 5$ WT, $n = 5$ TG; for females: $p = 0.4$, $F(1,8) = 0.77$, $n = 5$ WT, $n = 5$ TG). The overall magnitude of acoustic startle and PPI in our mice was also typical of that seen in the C57BL6/J background [167].

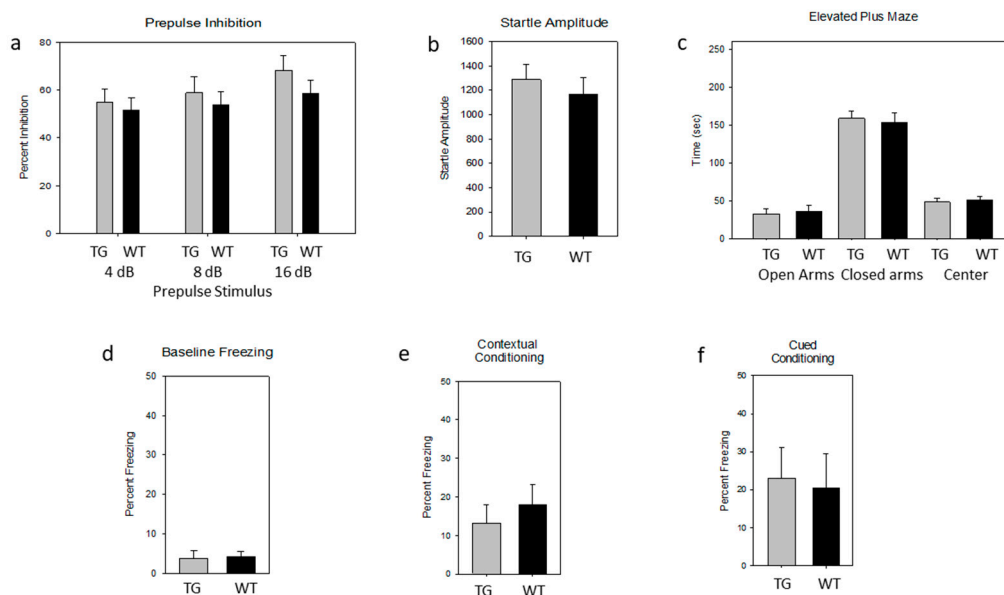


Figure 3. PDE4D5-D556A transgenic mice show no clear differences in prepulse inhibition, anxiety, or fear conditioning. Black bars: Wild-type (WT). Grey bars: PDE4D5-D556A (TG). Sexes are pooled. Data are means \pm SE. (a) Prepulse inhibition, percent inhibition with progressive stimulus (percent inhibition at prepulses of 4, 8, and 16 dB over background). (b) Prepulse inhibition, amplitude of startle response. (c) Elevated plus maze, time in each arm. (d) Fear conditioning, baseline freezing. (e) Fear conditioning, contextual conditioning. (f) Fear conditioning, cued conditioning.

2.5. Lack of an Effect of the PDE4D5-D556A Transgene on Tests of Anxiety

We used the elevated plus maze to assess for a potential anxiogenic effect of the PDE4D5-D556A transgene. We tested both the time spent in the open arms (Figure 3c) and exploration attempts.

PDE4D5-D556A transgenic mice, compared to their wild-type littermates, spent indistinguishable amounts of time in each arm (TG vs. WT, sexes pooled: $p = 0.54$, $F(9,1) = 0.40$ for closed arms; $p = 0.69$, $F(9,1) = 0.164$ open arms; $p = 0.58$, $F(9,1) = 0.32$ for center, $n = 10$ WT, $n = 10$ TG), with no detectable difference by sex (females: $p = 0.87$, $F(4,1) = 0.0289$ for closed arms; $p = 0.82$, $F(4,1) = 0.055$ for open arms; $p = 0.98$, $F(4,1) = 0.008$ for center, $n = 5$ WT, $n = 5$ TG; males: $p = 0.49$, $F(4,1) = 0.56$ for closed arms; $p = 0.78$, $F(4,1) = 0.09$ for open arms; $p = 0.46$, $F(4,1) = 0.66$ for center, $n = 5$ WT, $n = 5$ TG).

2.6. Lack of an Effect of the PDE4D5-D556A Transgene on Fear-Associated Conditioning

PDE4-selective inhibitors have potential therapeutic value in disorders of human learning and memory (see background). A defect in fear-associated conditioning is a hallmark of mice deficient in CREB [65,66,168–172], a PKA substrate that is regulated in part by PDEs [49,50]. Therefore, we tested PDE4D5-D556A transgenic and wild-type mice in a typical fear-associated conditioning protocol, with measurement of the baseline freezing (Figure 3d) and both context-dependent and cue-dependent conditioning (Figure 3e,f). We found no detectable difference between PDE4D5-D556A transgenic and wild-type mice in baseline freezing (i.e., prior to the presentation of the cue; Figure 3d; percent freezing, TG vs. WT, sexes pooled: $p = 0.85$, $F(8,1) = 0.04$, $n = 9$ WT, $n = 9$ TG; for males: $p = 0.29$, $F(3,1) = 1.68$, $n = 5$ WT, $n = 4$ TG; for females: $p = 0.97$, $F(3,1) = 0.001$, $n = 4$ WT, $n = 5$ TG). We also detected no difference in freezing on exposure to a novel context after contextual conditioning (Figure 3e; percent freezing, sexes pooled: $p = 0.40$, $F(9,1) = 0.78$, $n = 10$ WT, $n = 10$ TG; for males: $p = 0.56$, $F(4,1) = 0.40$; $n = 5$ WT, $n = 5$ TG; for females: $p = 0.59$, $F(4,1) = 0.33$, $n = 5$ WT, $n = 5$ TG). We also detected no difference in freezing after cued conditioning (Figure 3f; percent freezing with stimulus, sexes pooled: $p = 0.80$, $F(9,1) = 0.07$; $n = 10$ WT, $n = 10$ TG; for males: $p = 0.74$, $F(4,1) = 0.12$, $n = 5$ WT, $n = 5$ TG; for females: $p = 0.46$, $F(4,1) = 0.66$, $n = 5$ WT, $n = 5$ TG).

2.7. Effects of the PDE4D5-D556A Transgene on Spatial Learning

Spatial learning is dependent, at least in part, on hippocampal function and is defective in mice with mutations in CREB [65,66,168–172] and mutations in other elements of cAMP signaling pathways, including adenylyl cyclase [173] and Epac [174,175]. Therefore, we assessed the effects of the PDE4D5-D556A transgene on spatial learning, using the Morris water maze [176]. Male PDE4D5-D556A transgenic mice demonstrated significant impairment in spatial learning, in that their time to reach the target in the water maze was significantly longer than for wild-type mice (Figure 4a). This effect was detectable on days 4 and 5 of the typical 5-day training protocol (values for the entire 5-day training period: $p = 0.21$, $F(4,1) = 2.20$; values for days 4 and 5 only: $p = 0.038$, $F(1,1) = 273.3$, $n = 9$ WT, $n = 9$ TG). Female PDE4D5-D556A transgenic mice performed differently from their male counterparts in this assay, in that they performed better initially but then seemed to learn at a slower rate overall, so that their overall performance was undistinguishable statistically from wild-type females (Figure 4b, values for the entire 5-day training period: $p = 0.87$, $F(4,1) = 0.02$, values for days 4 and 5 only: $p = 0.29$, $F(1,1) = 7.11$, $n = 8$ WT, $n = 10$ TG). However, when the data from each female genotype were normalized relative to its own day 1 performance, a statistically significant difference was seen on subsequent days ($p = 0.0196$, $F(4,1) = 14.20$). When data for sexes were pooled, the differences on days 4 and 5 were more discernable (Figure 4c, values for the entire 5-day training period: $p = 0.42$, $F(9,1) = 0.71$, values for days 4 and 5 only: $p = 0.0073$, $F(3,1) = 42.56$, $n = 20$ WT, $n = 20$ TG). In this assay, male mice swam somewhat more slowly than females, but there was no discernable difference in the swimming distance between wild-type and PDE4D5-D556A transgenic mice (i.e., distance traveled to reach the target, TG males, 18.93 ± 1.13 ; WT males, 19.84 ± 1.30 , TG females, 20.59 ± 0.90 ; WT females, 20.12 ± 1.20 ; all means \pm SEM, $p = \text{NS}$). Testing the performance of the mice to remember the correct quadrant, after 5 days of testing and upon removal of the target platform, showed significant variability, with no statistical significance seen (probe trials, Figure 4d, comparing quadrant A to quadrant R, sexes pooled, $p = 0.087$, $F = (1,31)3.11$, $n = 16$ TG, $n = 17$ WT).

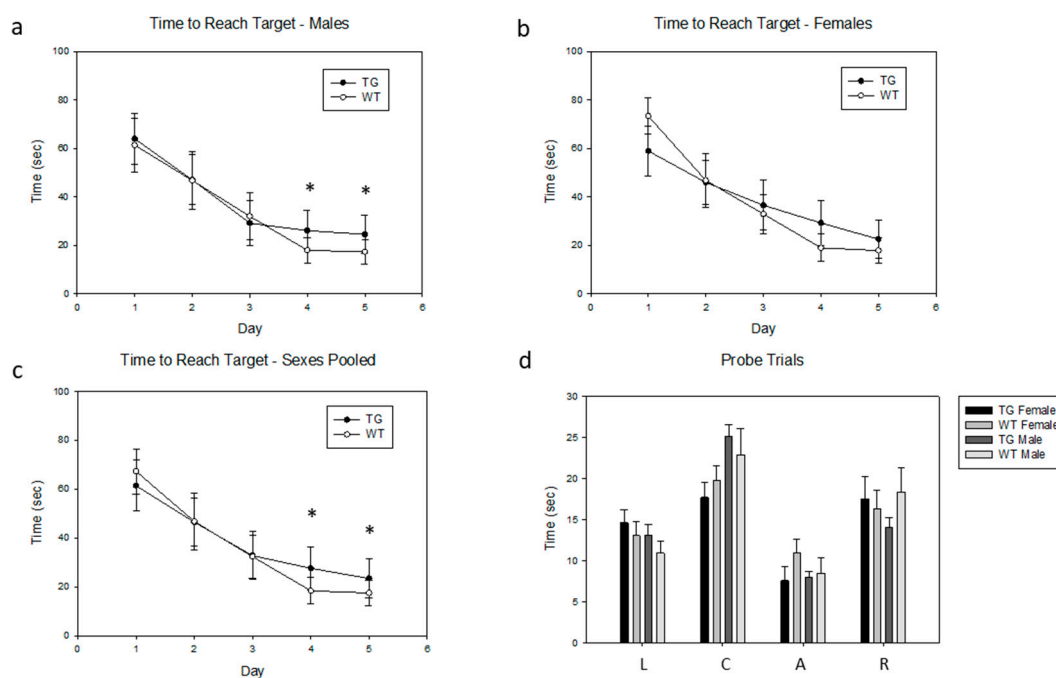


Figure 4. PDE4D5-D556A male mice show increased latency (time to target) in the Morris water maze. Data are means \pm SE; asterisks (*) indicate data from the transgenic mice that were statistically different over days 4 and 5 from that obtained from wild-type mice. (a) Time to reach target during the training phase, males. (b) Time to reach target during the training phase, females. (c) Time to reach target during the training phase, sexes pooled. (d) Probe trials: time spent in each quadrant for each genotype and sex. L: left quadrant; C: contralateral quadrant; A: quadrant that previously contained the target; R: right quadrant.

3. Discussion

We developed transgenic mice that express a dominant-negative mutant (D556A) of a single PDE4 isoform, specifically PDE4D5, preferentially in the hippocampus and forebrain and shown that the transgene produces significant effects on behavior. The use of a dominant-negative transgene in this study, and in our prior study of PDE4B1 [133], is a novel approach to determining the functions of PDE4 isoforms in the CNS. Previously, studies of PDE4 function employed gene knockouts [27,137–143], lentiviral siRNA [142,144–147], or dominant-negative mutants encoded by adenoviruses [135,136]. We developed this approach after we and our collaborators carefully studied the effects of the PDE4D5-D566A mutant in cell-based assays [103,108,109], as described in more detail below. Based on the cell-based studies, and our prior experience with PDE4B1 [133], we felt that this mutant, when expressed as a transgene, would have a more isoform-selective effect than that seen in prior studies of *Pde4d* gene knockouts. An important reason for this prediction is that the mouse *Pde4d* and human *PDE4D* gene both encode 11 isoforms (Figure 1a; [73,88,96–100]), each with a distinct amino acid sequence and distribution in tissues. For this reason, *Pde4d*^{-/-} mice have a phenotype that reflects the combined deficiency of all 11 PDE4D isoforms, which prevents analysis of the effect(s) of any individual isoform, such as PDE4D5. For this reason, our approach is likely to have greater selectivity for the PDE4D5 isoform than *Pde4d*^{-/-} gene knockouts or siRNA. Our dominant-negative approach also follows the strategy used by several groups to study PKA and CREB in the CNS, in that transgenic mice expressing a dominant-negative PKA RI α subunit [177], or a dominant-negative CREB mutant [32,66,169–171,178–180], all have defects in various components of learning and memory.

We emphasize PDE4D5 for several reasons. First, human PDE4D5 (GenBank AF012073) and mouse PDE4D5 (GenBank XP_006517707.1) are extremely similar, being identical in length and having a 98% amino acid identity. Secondly, PDE4D5 mRNA is expressed in several regions of the mouse CNS

(see background for details), compatible with it being targeted by a transgene driven by the α CaMKII promoter. Finally, PDE4D5 interacts with several proteins, most notably RACK1 and β -arrestin2, both of which appear to have a much higher selectivity and avidity for PDE4D5 than for any other PDE4 isoform (see background for references). In particular, PDE4D5 appears to have a pivotal role in regulating signaling through the β_2 -adrenergic receptor [108,109,111,112,148,149]. Therefore, study of PDE4D5 might provide insights into the role(s) of β_2 -adrenergic signaling in the CNS.

In the current study, the PDE4D5-D556A-encoding transgene was expressed off the α CaMKII promoter [155–157]. We also used this promoter in a recent prior study to express a dominant-negative mutant of PDE4B1 [133]. We chose this promoter as it is active preferentially in forebrain excitatory neurons, including those in the hippocampus, amygdala, cortex, and striatum [155,156]. This choice may also minimize any effects of the transgene on prenatal development, as the α CaMKII promoter becomes active several days after birth [181], when many CNS pathways are already formed [157]. This promoter has been employed in the development of knockout and transgenic mice used in many studies of learning and memory [155,157,169–171,177,182–184] and other neurobiological phenotypes [185]. However, given the differences in the regional expression of α CaMKII and PDE4D5, we do not expect that all of the biological functions of PDE4D5 are disrupted equally in all areas of the brain where it is normally expressed. Additionally, the expression of the transgene may vary according to its insertion site. Our PDE4D5-D556A-encoding transgene is likely to be expressed in brain areas lacking endogenous PDE4D5; however, since extensive study of PDE4D5-D556A in cell-based assays has shown that all of its biological effects are mediated through its action on endogenous PDE4D5, as described in the next three paragraphs, the transgene is unlikely to have a meaningful biological effect in those areas.

When overexpressed, the PDE4D5-D556A protein produces no change in the total PDE4 enzymatic activity in cell-based systems. Instead, it disrupts PDE4D5 cellular function in a dominant-negative fashion by producing an equilibrium displacement of endogenous PDE4D5 from its protein partner(s), most notably RACK1 and β -arrestin2 [103,108,109,111,132]. Although an “off-target” effect of the PDE4D5-D556A protein on other PDE4 isoforms, notably other PDE4D isoforms, cannot be excluded completely, we believe this is unlikely, as PDE4D5 interacts highly selectively with different protein partners than other PDE4D isoforms do (see background for details). Therefore, the expression of PDE4D5-D556A should block PDE4D5 function in specific sub-cellular compartments where PDE4D5 is active, increase cAMP levels, and ultimately activate PKA. Activation of PKA is likely to lead to increased phosphorylation of CREB, a major PKA substrate, in regions of the CNS where our transgene is expressed, including area CA1 of the hippocampus and the dentate gyrus. Some effects of the transgene may also be mediated by other cAMP effectors, including EPAC [68,174,175] and/or cyclic nucleotide-gated ion channels [70]. This model of PDE4D5-D556A action does not require that global levels of cAMP change detectably with the PDE4D5-D556A-encoding transgene. Instead, tissue-level cAMP levels would reflect the cumulative effect of numerous elements in cAMP signaling, including the effects (potentially compensatory) of other PDE4 isoforms, as well as the effects of members of other PDE families. Indeed, it is conceivable, although not likely, that PDE4D5-D556A could lower cAMP levels in certain contexts, e.g., by shifting endogenous PDE4D5 into a subcellular compartment where it is not normally present.

It is possible that some of the effects of PDE4D5-D556A are mediated by its ability to interfere with the homodimerization of PDE4D5 [107,127–131]. This is because PDE4D5 interacts with β -arrestin2 only when PDE4D5 is monomeric [107]. Therefore, PDE4D5-D556A can act as a dominant-negative in two ways: (1) It can compete, as a monomer, with monomeric wild-type PDE4D5 for interaction with β -arrestin2, by binding directly to β -arrestin2; or (2) It can dimerize with wild-type PDE4D5; the resulting dimer does not interact with β -arrestin2. We did not detect any “off-target” effects of PDE4D5-D556A in these studies, as heterodimerization of PDE4 isoforms has not been observed [107, 127], although it cannot be definitely excluded in the studies that have been performed to date.

Some of the effects of PDE4D5-D556A may be mediated through its effects on RACK1 and β -arrestin2, or other proteins that interact selectively with PDE4D5. By dramatically increasing scaffold sites for β -arrestin2 and RACK1, PDE4D5-D556A may sequester these proteins and thereby block their normal functions in cells. This effect would produce a CNS phenotype that would differ from that seen with pharmacological inhibition of PDE4D5, and especially from that seen with small-molecule inhibitors of the catalytic activity of PDE4D5. Such a mechanism might explain some of the behavioral effects that we see in our transgenic mice, as explained in more detail in the next paragraph.

Our PDE4D5-D556A transgenic mice have a phenotype that seems to affect hippocampal-dependent positional learning (place preference), based on their performance in the Morris water maze [176]. This result is consistent with prior studies that show that cAMP signaling mediated by CREB, and/or possibly EPAC, plays an essential role in learning and memory (see [64–66,68,69] for reviews). However, the direction and magnitude of the effect that we observed were intriguing. Given that PDE4 inhibitors are being developed as enhancers of cognition and memory, we were expecting that attenuation of PDE4 activity in the brain would produce an enhancement of performance in tests of learning and memory. However, our PDE4D5-D556A mutant appeared to produce a deleterious effect in the Morris water maze. Although the mechanism(s) of this paradoxical effect are uncertain, it is possible that it reflects the ability of PDE4D5-D556A to sequester RACK1 and/or β -arrestin2, as described above. Although further experiments are necessary to support this hypothesis, our data clearly support a role for PDE4D5 and its specific partner proteins in hippocampal-dependent learning and memory.

In our studies, the PDE4D5-D556A transgene had no detectable effect on associative fear conditioning. Fear conditioning, especially contextual fear conditioning, was tested because it is an amygdala-dependent memory test mediated, at least in part, by CREB action in the hippocampus [65,66,168–172]. One potential reason for our results is the notably high baseline performance of wild-type C57BL/6J mice in this assay, which meant that any improvement in the transgenic mice might have been obscured, especially when strong stimuli were used in conditioning, as we did here. A weak effect in this assay might also have been missed because of the sample size; however, sample sizes were limited by animal ethics issues and financial resources. Finally, our PDE4D5-D556A transgene may not have been expressed at sufficiently high levels in the amygdala to suppress the action of endogenous PDE4D5 in this area.

Given their phenotype in the open-field test, our PDE4D5-D556A transgenic mice appear to have a behavioral phenotype that affects activity. This effect was clearly sex dependent, in that transgenic females were less active than wild-type females, while transgenic males had a tendency to be more active than wild-type males. Overall, however, the PDE4D5-D556A transgene had a weaker effect in males than the PDE4B1-D564A transgene, which produced a highly significant increase in the activity of males in the open-field test [133]. The potential neurophysiological mechanism(s) and/or anatomical site(s) of action for these sex differences is not certain; it is possible that there are sex-dependent differences in the expression of the transgene, although this has not been reported previously for transgenes expressed off the α CaMKII promoter [155–157]. Nonetheless, these data demonstrate clearly that PDE4B1 and PDE4D5 have significantly different functional roles in the CNS and that our dominant-negative approach clearly has sufficient isoform selectivity to distinguish between these differing functional roles. As PDE4D5-D556A transgenic mice had behavior indistinguishable from wild-type mice in the elevated plus maze, we also conclude that the PDE4D5-D556A transgene does not appear to have an anxiogenic effect.

Two different groups have studied the behavioral phenotypes of *Pde4d*^{-/-} mice [27,137,142]. Some of these studies show that *Pde4d*^{-/-} mice have behavior that mimics the effects of some antidepressants [137], for example, decreased immobility in forced-swim and tail-suspension tests. One group has concluded that *Pde4d*^{-/-} mice do better in tests of learning and memory [142], while another group, studying an apparently identical genotype, did not detect this effect [27]. Comparing these data to those in the present study is complicated further by the fact that *Pde4d*^{-/-} mice appear to have phenotypes

that are affected by processes in areas of the brain, notably the striatum, beyond those in the forebrain/hippocampus, which was the focus of the present study. Finally, all *Pde4* knockouts have significant non-CNS phenotypes [186,187], such as slow growth, small adult size, and impaired fertility. The differences between the findings in the present study and those obtained by these two groups with *Pde4d*^{-/-} mice probably also reflect isoform differences (PDE4D5 vs. all PDE4D isoforms). Differences in assay conditions, genetic background, age at the time of study, or other factors could also be responsible.

In humans, a specific set of mutations in *PDE4D* cause acrodysostosis, a disorder that affects bone formation [188–192]. Patients with acrodysostosis and *PDE4D* mutations also have significant intellectual disability. Acrodysostosis mutations cluster in a specific region of the PDE4D protein that is essential for its dimerization and regulation by phosphorylation by PKA [127]. Unlike our PDE4D5-D556A mutant, acrodysostosis mutations do not affect amino acids that are directly involved in catalysis [127]. The CNS deficiencies that are seen in acrodysostosis appear to be considerably more severe than those seen in *Pde4d*^{-/-} or PDE4D5-D556A transgenic mice, affecting multiple aspects of cognition and memory. It is uncertain whether this reflects a purely species difference or a different mutation mechanism (unlike our dominant-negative PDE4D5-D556A mutant, the *PDE4D* acrodysostosis mutants appear to have a “gain-of-function” effect, in that they render the enzyme constitutively insensitive to PKA regulation). Although much remains to be learned about the CNS phenotypes of *PDE4D*-mutant acrodysostosis, the available data demonstrate the profound effects of PDE4D alterations in the CNS and thereby the essential role of PDE4D in CNS function in humans.

Our data, along with the observations from other groups summarized above, show convincingly that PDE4D5 has an important role in the CNS. Therefore, our results, and those of other groups, provide strong justification for the focusing on PDE4D, and PDE4D5 in particular, as a target for drug development [38,43,45–48,58,60,193–195]. Recent human trials of pan-selective PDE4 inhibitors active in the human CNS have shown some promise [9,10,12]. To date, the development of PDE4-selective inhibitors in many CNS indications has been limited by nausea and emesis [86]. Many of the emetogenic effects of PDE4 inhibitors are mediated by the area postrema, where several PDE4B and PDE4D isoforms are known to be expressed [82,196]. However, it should still be possible to target PDE4 isoforms or conformers that are not present in the area postrema, with potential value in the treatment of depression and disorders of learning and memory. Novel approaches to targeting these isoforms might include CRISPR or shRNA specific to each individual isoform, or small-molecule disruptors of the interaction of specific isoforms with their specific binding partner proteins.

4. Materials and Methods

4.1. Generation of Transgenic Mice

Transgenic mice expressing PDE4D5-D556A, under the control of the α -calmodulin kinase II (α CaMKII) promoter, were generated using methods that we described previously for dominant-negative PDE4B1 [133]. The PDE4D5-D556A mutant (Asp556Ala, GAC to GCC) in full-length human PDE4D5 (Figure 1c, GenBank AF012073, [88]), with sequences encoding an 11-amino-acid carboxyl-terminal VSV epitope [197], was generated by site-directed mutagenesis and cloned into the expression plasmid pMM403 ([155,156]; generously provided by Mark Mayford, Scripps Institute, La Jolla, CA, USA). All animal work was performed under protocols approved prior to the initiation of the study (Animal Project Number: 08010842) by the Institutional Animal Care and Use Committee (IACUC) of the University of Alabama at Birmingham and followed the NIH guide for the care and use of laboratory animals and other national regulations and policies. All efforts were made to minimize suffering and no surgery was performed.

4.2. Immunoblotting

Monkey COS-7 cells (purchased from ATCC, Manassas, VA, USA) were transfected with the plasmid pcDNAN79D556AVSV, or with vector pcDNA3 (Invitrogen, ThermoFisher, Carlsbad, CA,

USA), using technology that we described previously [198]. The plasmid pcDNAN79D556AVSV encodes human PDE4D5-D556A, with the carboxyl-terminal VSV epitope [197]. Extracts from COS-7 cells and brain, respectively, were prepared using techniques we described previously [133,198,199]. The extracts were subjected to LDS-PAGE (Novex, Invitrogen, ThermoFisher, USA) and immunoblotted. For comparing apparent molecular weights under denaturing conditions, samples were run in parallel lanes on the same gel and then transferred to a single filter for immunoblotting. The filter was then cut in half cross-wise, with the top half incubated with an antibody to VSV (mouse, clone P5D4, Millipore-Sigma, St. Louis, MO, USA, ref. [197], 1:5000) in Tris-buffered saline (TBS) with 0.1% Tween-20 and 0.5% non-fat dry milk for 1 h. As a loading control, the bottom half was incubated with an antibody to GAPDH (rabbit, clone D16H11, Cell Signaling Technologies [CST], Danvers, MA, USA, 1:2000), as for VSV, except that incubation was in Tris-buffered saline (TBS) with 0.1% Tween-20 and 5% non-fat dry milk for 24 h at 4 °C. Primary antibody incubations were then followed by 2 washes in TBS with 0.1% Tween-20. Secondary antibody incubations (mouse, SC-516102, Santa Cruz Biotechnology, Santa Cruz, CA, USA, 1:5000; rabbit, CST 7074, 1:5000) were performed in the same buffer, followed by 3 washes in the same buffer. Signals were developed with ECL (Pierce, ThermoFisher, USA). Imaging was performed with a C-DIGIT scanner and ImageStudio software, version 5.2 (LI-COR Biosciences, Lincoln, NE, USA).

4.3. Behavioral Assays

Mice were tested at 8–12 weeks of age. Mice were housed in cages containing 2 to 5 animals on a 12-h light:12-h dark cycle, with all behavioral testing performed in the light phase. The experimenter was blind to the genotype of the mice during testing and data collection/analysis. Testing for the basic neurobiology (SHIRPA) battery was performed on cohort 1 (2 generations backcrossed into C57BL/6J). Open-field testing, followed about 7 days later by fear conditioning and then acoustic startle, and then followed about 7 days later by the elevated plus maze and the Morris water maze, were performed on a separate cohort (cohort 2; 3 generations back-crossed into C57BL/6J). Testing in the Morris water maze was then performed on a third cohort (cohort 3; 4 generations backcrossed into C57BL/6J) and the results pooled with those from cohort 2. For each experiment, sample sizes were determined after review of the previously published descriptions of each procedure (for details, see the references cited in Sections 4.4–4.9). Males and females were tested throughout and results (WT vs. TG) were analyzed separately for each sex. In addition, the results for both sexes were pooled, and statistical tests performed on this pooled sample set. For all behavioral assays, data were collected in Excel 2013 (Microsoft, Redmond, WA, USA) and statistical analysis and graphs prepared with SigmaPlot 12.0 (Systat, San Jose, CA, USA).

4.4. Basic Neurobiological Battery

This was performed according to the SHIRPA protocol [158,159], as we described previously [133].

4.5. Open-Field Testing

This was performed using a photobeam apparatus [167,200,201], as we described previously [133].

4.6. Acoustic Startle and Prepulse Inhibition

This was performed using a dedicated apparatus [167,202], as we described previously [133].

4.7. Elevated Plus Maze

This test, a standard test for measuring anxiety-like behavior [203], was performed as we described previously [133].

4.8. Context-Dependent and Cue-Dependent Fear Conditioning

This was performed as described previously by numerous groups [167,200,201,204–207] and exactly as reported previously by us [133].

4.9. Morris Water Maze

The Morris water maze test [176] measures the ability of an animal to recall the position of a hidden platform (i.e., the escape platform) upon training. Therefore, responses were measured after a series of training steps. Mice were trained in a 120-cm blue circular pool containing clear water and a 10-cm round escape platform located 0.5 cm below the water surface. Water temperature was maintained at 20–22 °C. Mice were placed into the water facing the wall, in different quadrants on a random basis, and allowed to search for the platform for 60 s. If the mice did not locate the platform at the end of 60 s, they were guided to it. The mice were permitted to stay on the platform for 10 s and then were returned to their cages. All trials were performed at the same time of day (± 1 h) during the animals' light phase. Each mouse was given two blocks of 4 trials a day for 5 consecutive days, with a 20-min inter-trial interval. For probe trials (i.e., response assessment), which were performed on day 5, each mouse was placed in the pool in the absence of the escape platform and its search monitored for 60 s. The movements of the mice during training and in the probe trials were recorded by a continuous video tracking system (Ethovision, Noldus, The Netherlands) and analyzed using Hvswater. During training sessions, the time (i.e., escape latency) and distance for the mouse to locate the platform were recorded. During the probe trial, the time spent searching each quadrant (quadrant search time) was recorded. Escape latency and distance data were analyzed with a two-way (genotype \times trial block) ANOVA with repeated measures. Search time was analyzed with a one-way ANOVA.

4.10. Availability of Data and Materials

The datasets used and/or analysed during the current study are available from the corresponding author on reasonable request.

Author Contributions: G.B.B. provided overall supervision and planned and performed many of the behavioral experiments. T.v.G. performed and interpreted the Morris water maze and plus maze experiments. L.H.M.S. performed transfections and genotyping. All experiments were performed at the University of Alabama at Birmingham, except for the immunoblotting described in Figure 1d, which was performed by G.B.B. at BZI Pharma LLC. All authors have read and agreed to the published version of the manuscript.

Funding: The McKnight Foundation (no grant number, for research support and also funding of the behavioral cores), the Bolger Prostate Cancer Research Fund (no grant number), and the National Cancer Institute of the National Institutes of Health, USA, to the University of Alabama at Birmingham Comprehensive Cancer Center under award number P30 CA013148 (for generation of transgenic mice and DNA sequencing). The content is solely the responsibility of the authors and does not necessarily represent the official views of the National Institutes of Health, the McKnight Foundation, or BZI Pharma LLC, none of which played any role on the in study design; in the collection, analysis, and interpretation of data; in the writing of the manuscript; or in the decision to submit the manuscript for publication.

Acknowledgments: We thank Mark Mayfield for providing plasmids; he has agreed to be acknowledged solely for this purpose.

Conflicts of Interest: Graeme Bolger is the founder of, and holds an ownership interest in, BZI Pharma LLC. Otherwise, the authors certify that they have no conflict of interest.

References

1. Fleischhacker, W.W.; Hinterhuber, H.; Bauer, H.; Pflug, B.; Berner, P.; Simhandl, C.; Wolf, R.; Gerlach, W.; Jaklitsch, H.; Sastre-y-Hernandez, M.; et al. A multicenter double-blind study of three different doses of the new cAMP-phosphodiesterase inhibitor rolipram in patients with major depressive disorder. *Neuropsychobiology* **1992**, *26*, 59–64. [[CrossRef](#)] [[PubMed](#)]
2. Scott, A.I.; Perini, A.F.; Shering, P.A.; Whalley, L.J. In-patient major depression: Is rolipram as effective as amitriptyline? *Eur. J. Clin. Pharmacol.* **1991**, *40*, 127–129. [[PubMed](#)]

3. Krause, W.; Kuhne, G.; Sauerbrey, N. Pharmacokinetics of (+)-rolipram and (-)-rolipram in healthy volunteers. *Eur. J. Clin. Pharmacol.* **1990**, *38*, 71–75. [[CrossRef](#)] [[PubMed](#)]
4. Hebenstreit, G.F.; Fellerer, K.; Fichte, K.; Fischer, G.; Geyer, N.; Meya, U.; Hernandez, M.; Schony, W.; Schratzer, M.; Soukop, W.; et al. Rolipram in major depressive disorder: Results of a double-blind comparative study with imipramine. *Pharmacopsychiatry* **1989**, *22*, 156–160. [[CrossRef](#)]
5. Eckmann, F.; Fichte, K.; Meya, U. Rolipram in major depression: Results of a double-blind comparative study with amitriptyline. *Curr. Ther. Res.* **1988**, *43*, 291–295.
6. Horowski, R.; Sastre-Y-Hernandez, M. Clinical effects of the neurotropic selective cAMP phosphodiesterase inhibitor rolipram in depressed patients: Global evaluation of the preliminary reports. *Curr. Ther. Res.* **1985**, *38*, 23–29.
7. Bobon, D.; Breulet, M.; Gerard-Vandenhove, M.A.; Guiot-Goffioul, F.; Plomteux, G.; Sastre-y-Hernandez, M.; Schratzer, M.; Troisfontaines, B.; Von Frenckell, R.; Wachtel, H. Is phosphodiesterase inhibition a new mechanism of antidepressant action? A double blind double-dummy study between rolipram and desipramine in hospitalized major and/or endogenous depressives. *Eur. Arch. Psychiatry Neurol. Sci.* **1988**, *238*, 2–6. [[CrossRef](#)]
8. Zeller, E.; Stief, H.J.; Pflug, B.; Sastre-y-Hernandez, M. Results of a phase II study of the antidepressant effect of rolipram. *Pharmacopsychiatry* **1984**, *17*, 188–190. [[CrossRef](#)]
9. Van Duinen, M.A.; Sambeth, A.; Heckman, P.R.; Smit, S.; Tsai, M.; Lahu, G.; Uz, T.; Blokland, A.; Prickaerts, J. Acute administration of roflumilast enhances immediate recall of verbal word memory in healthy young adults. *Neuropharmacology* **2018**, *131*, 31–38. [[CrossRef](#)]
10. Heckman, P.R.; Van Duinen, M.A.; Blokland, A.; Uz, T.; Prickaerts, J.; Sambeth, A. Acute administration of roflumilast enhances sensory gating in healthy young humans in a randomized trial. *Psychopharmacology (Berl)* **2018**, *235*, 301–308. [[CrossRef](#)]
11. Prickaerts, J.; Heckman, P.R.; Blokland, A. Investigational phosphodiesterase inhibitors in phase I and phase II clinical trials for Alzheimer's disease. *Expert Opin. Investig. Drugs* **2017**, *26*, 1033–1048. [[CrossRef](#)] [[PubMed](#)]
12. Prickaerts, J.; Heckman, P.R.; Blokland, A. Acute treatment with the PDE4 inhibitor roflumilast improves verbal word memory in healthy old individuals: A double-blind placebo-controlled study. *Neurobiol. Aging* **2019**, *77*, 37–43. [[CrossRef](#)]
13. Wachtel, H. Potential antidepressant activity of rolipram and other selective cyclic adenosine 3',5'-monophosphate phosphodiesterase inhibitors. *Neuropharmacology* **1983**, *22*, 267–272. [[CrossRef](#)]
14. Wachtel, H.; Schneider, H.H. Rolipram, a novel antidepressant drug, reverses the hypothermia and hypokinesia of monoamine-depleted mice by an action beyond postsynaptic monoamine receptors. *Neuropharmacology* **1986**, *25*, 1119–1126. [[CrossRef](#)]
15. Barad, M.; Bourtchouladze, R.; Winder, D.G.; Golan, H.; Kandel, E. Rolipram, a type IV-specific phosphodiesterase inhibitor, facilitates the establishment of long-lasting long-term potentiation and improves memory. *Proc. Natl. Acad. Sci. USA* **1998**, *95*, 15020–15025. [[CrossRef](#)]
16. Bach, M.E.; Barad, M.; Son, H.; Zhuo, M.; Lu, Y.F.; Shih, R.; Mansuy, I.; Hawkins, R.D.; Kandel, E.R. Age-related defects in spatial memory are correlated with defects in the late phase of hippocampal long-term potentiation in vitro and are attenuated by drugs that enhance the cAMP signaling pathway. *Proc. Natl. Acad. Sci. USA* **1999**, *96*, 5280–5285. [[CrossRef](#)]
17. Titus, D.J.; Sakurai, A.; Kang, Y.; Furones, C.; Jergova, S.; Santos, R.; Sick, T.J.; Atkins, C.M. Phosphodiesterase inhibition rescues chronic cognitive deficits induced by traumatic brain injury. *J. Neurosci.* **2013**, *33*, 5216–5226. [[CrossRef](#)]
18. Mueller, E.M.; Hofmann, S.G.; Cherry, J.A. The type IV phosphodiesterase inhibitor rolipram disturbs expression and extinction of conditioned fear in mice. *Neuropharmacology* **2010**, *59*, 1–8. [[CrossRef](#)]
19. Nibuya, M.; Nestler, E.J.; Duman, R.S. Chronic antidepressant administration increases the expression of cAMP response element binding protein (CREB) in rat hippocampus. *J. Neurosci.* **1996**, *16*, 2365–2372. [[CrossRef](#)]
20. Zhong, P.; Wang, W.; Yu, F.; Nazari, M.; Liu, X.; Liu, Q.S. Phosphodiesterase 4 inhibition impairs cocaine-induced inhibitory synaptic plasticity and conditioned place preference. *Neuropsychopharmacology* **2012**, *37*, 2377–2387. [[CrossRef](#)]

21. Villiger, J.W.; Dunn, A.J. Phosphodiesterase inhibitors facilitate memory for passive avoidance conditioning. *Behav. Neural Biol.* **1981**, *31*, 354–359. [[CrossRef](#)]
22. Thompson, B.E.; Sachs, B.D.; Kantak, K.M.; Cherry, J.A. The Type IV phosphodiesterase inhibitor rolipram interferes with drug-induced conditioned place preference but not immediate early gene induction in mice. *Eur. J. Neurosci.* **2004**, *19*, 2561–2568. [[CrossRef](#)] [[PubMed](#)]
23. Zhang, H.T.; Zhao, Y.; Huang, Y.; Dorairaj, N.R.; Chandler, L.J.; O'Donnell, J.M. Inhibition of the phosphodiesterase 4 (PDE4) enzyme reverses memory deficits produced by infusion of the MEK inhibitor U0126 into the CA1 subregion of the rat hippocampus. *Neuropsychopharmacology* **2004**, *29*, 1432–1439. [[CrossRef](#)] [[PubMed](#)]
24. Rutten, K.; Prickaerts, J.H.; Blokland, A. Rolipram reverses scopolamine-induced and time-dependent memory deficits in object recognition by different mechanisms of action. *Neurobiol. Learn. Mem.* **2006**, *85*, 132–138. [[CrossRef](#)] [[PubMed](#)]
25. Zhang, H.T.; Zhao, Y.; Huang, Y.; Deng, C.; Hopper, A.T.; De Vivo, M.; Rose, G.M.; O'Donnell, J.M. Antidepressant-like effects of PDE4 inhibitors mediated by the high-affinity rolipram binding state (HARBS) of the phosphodiesterase-4 enzyme (PDE4) in rats. *Psychopharmacology (Berl)* **2006**, *186*, 209–217. [[CrossRef](#)] [[PubMed](#)]
26. Rutten, K.; Basile, J.L.; Prickaerts, J.; Blokland, A.; Vivian, J.A. Selective PDE inhibitors rolipram and sildenafil improve object retrieval performance in adult cynomolgus macaques. *Psychopharmacology (Berl)* **2008**, *196*, 643–648. [[CrossRef](#)] [[PubMed](#)]
27. Rutten, K.; Misner, D.L.; Works, M.; Blokland, A.; Novak, T.J.; Santarelli, L.; Wallace, T.L. Enhanced long-term potentiation and impaired learning in phosphodiesterase 4D-knockout (PDE4D) mice. *Eur. J. Neurosci.* **2008**, *28*, 625–632. [[CrossRef](#)]
28. Kanos, S.J.; Tokarczyk, J.; Siegel, S.J.; Bilker, W.; Abel, T.; Kelly, M.P. Rolipram: A specific phosphodiesterase 4 inhibitor with potential antipsychotic activity. *Neuroscience* **2007**, *144*, 239–246. [[CrossRef](#)]
29. Rutten, K.; Prickaerts, J.; Schaenzle, G.; Rosenbrock, H.; Blokland, A. Sub-chronic rolipram treatment leads to a persistent improvement in long-term object memory in rats. *Neurobiol. Learn. Mem.* **2008**, *90*, 569–575. [[CrossRef](#)]
30. Li, Y.F.; Huang, Y.; Amsdell, S.L.; Xiao, L.; O'Donnell, J.M.; Zhang, H.T. Antidepressant- and anxiolytic-like effects of the phosphodiesterase-4 inhibitor rolipram on behavior depend on cyclic AMP response element binding protein-mediated neurogenesis in the hippocampus. *Neuropsychopharmacology* **2009**, *34*, 2404–2419. [[CrossRef](#)]
31. Rutten, K.; Van Donkelaar, E.L.; Ferrington, L.; Blokland, A.; Bollen, E.; Steinbusch, H.W.; Kelly, P.A.; Prickaerts, J.H. Phosphodiesterase inhibitors enhance object memory independent of cerebral blood flow and glucose utilization in rats. *Neuropsychopharmacology* **2009**, *34*, 1914–1925. [[CrossRef](#)] [[PubMed](#)]
32. Vecsey, C.G.; Baillie, G.S.; Jaganath, D.; Havekes, R.; Daniels, A.; Wimmer, M.; Huang, T.; Brown, K.M.; Li, X.Y.; Descalzi, G.; et al. Sleep deprivation impairs cAMP signalling in the hippocampus. *Nature* **2009**, *461*, 1122–1125. [[CrossRef](#)] [[PubMed](#)]
33. Cheng, Y.F.; Wang, C.; Lin, H.B.; Li, Y.F.; Huang, Y.; Xu, J.P.; Zhang, H.T. Inhibition of phosphodiesterase-4 reverses memory deficits produced by Abeta25-35 or Abeta1-40 peptide in rats. *Psychopharmacology (Berl)* **2010**, *212*, 181–191. [[CrossRef](#)] [[PubMed](#)]
34. Wang, C.; Yang, X.M.; Zhuo, Y.Y.; Zhou, H.; Lin, H.B.; Cheng, Y.F.; Xu, J.P.; Zhang, H.T. The phosphodiesterase-4 inhibitor rolipram reverses Abeta-induced cognitive impairment and neuroinflammatory and apoptotic responses in rats. *Int. J. Neuropsychopharmacol.* **2012**, *15*, 749–766. [[CrossRef](#)] [[PubMed](#)]
35. Werenicz, A.; Christoff, R.R.; Blank, M.; Jobim, P.F.; Pedroso, T.R.; Reolon, G.K.; Schroder, N.; Roesler, R. Administration of the phosphodiesterase type 4 inhibitor rolipram into the amygdala at a specific time interval after learning increases recognition memory persistence. *Learn. Mem.* **2012**, *19*, 495–498. [[CrossRef](#)] [[PubMed](#)]
36. Wiescholleck, V.; Manahan-Vaughan, D. PDE4 inhibition enhances hippocampal synaptic plasticity in vivo and rescues MK801-induced impairment of long-term potentiation and object recognition memory in an animal model of psychosis. *Transl. Psychiatry* **2012**, *2*, e89. [[CrossRef](#)]

37. Vanmierlo, T.; Creemers, P.; Akkerman, S.; van Duinen, M.; Sambeth, A.; De Vry, J.; Uz, T.; Blokland, A.; Prickaerts, J. The PDE4 inhibitor roflumilast improves memory in rodents at non-emetic doses. *Behav. Brain Res.* **2016**, *303*, 26–33. [[CrossRef](#)]
38. Zhang, C.; Xu, Y.; Zhang, H.T.; Gurney, M.E.; O'Donnell, J.M. Comparison of the Pharmacological Profiles of Selective PDE4B and PDE4D Inhibitors in the Central Nervous System. *Sci. Rep.* **2017**, *7*, 40115. [[CrossRef](#)]
39. Wang, C.; Zhang, J.; Lu, Y.; Lin, P.; Pan, T.; Zhao, X.; Liu, A.; Wang, Q.; Zhou, W.; Zhang, H.T. Antidepressant-like effects of the phosphodiesterase-4 inhibitor etazolate and phosphodiesterase-5 inhibitor sildenafil via cyclic AMP or cyclic GMP signaling in mice. *Metab. Brain Dis.* **2014**, *29*, 673–682. [[CrossRef](#)]
40. Liu, X.; Hao, P.D.; Yang, M.F.; Sun, J.Y.; Mao, L.L.; Fan, C.D.; Zhang, Z.Y.; Li, D.W.; Yang, X.Y.; Sun, B.L.; et al. The phosphodiesterase-4 inhibitor roflumilast decreases ethanol consumption in C57BL/6J mice. *Psychopharmacology (Berl)* **2017**, *234*, 2409–2419. [[CrossRef](#)]
41. Zhong, Y.; Zhu, Y.; He, T.; Li, W.; Yan, H.; Miao, Y. Rolipram-induced improvement of cognitive function correlates with changes in hippocampal CREB phosphorylation, BDNF and Arc protein levels. *Neurosci. Lett.* **2016**, *610*, 171–176. [[CrossRef](#)] [[PubMed](#)]
42. Akar, F.; Mutlu, O.; Celikyurt, I.K.; Ulak, G.; Erden, F.; Bektas, E.; Tanyeri, P. Effects of rolipram and zaprinast on learning and memory in the Morris water maze and radial arm maze tests in naive mice. *Drug Res. (Stuttg)* **2015**, *65*, 86–90. [[CrossRef](#)] [[PubMed](#)]
43. Sierksma, A.S.; van den Hove, D.L.; Pfau, F.; Philippens, M.; Bruno, O.; Fedele, E.; Ricciarelli, R.; Steinbusch, H.W.; Vanmierlo, T.; Prickaerts, J. Improvement of spatial memory function in APPswe/PS1dE9 mice after chronic inhibition of phosphodiesterase type 4D. *Neuropharmacology* **2014**, *77*, 120–130. [[CrossRef](#)] [[PubMed](#)]
44. Titus, D.J.; Wilson, N.M.; Freund, J.E.; Carballosa, M.M.; Sikah, K.E.; Furones, C.; Dietrich, W.D.; Gurney, M.E.; Atkins, C.M. Chronic Cognitive Dysfunction after Traumatic Brain Injury Is Improved with a Phosphodiesterase 4B Inhibitor. *J. Neurosci.* **2016**, *36*, 7095–7108. [[CrossRef](#)] [[PubMed](#)]
45. Wilson, N.M.; Gurney, M.E.; Dietrich, W.D.; Atkins, C.M. Therapeutic benefits of phosphodiesterase 4B inhibition after traumatic brain injury. *PLoS ONE* **2017**, *12*, e0178013. [[CrossRef](#)] [[PubMed](#)]
46. Hedde, J.R.; Hanks, A.N.; Schmidt, C.J.; Hughes, Z.A. The isozyme selective phosphodiesterase-4 inhibitor, ABI-4, attenuates the effects of lipopolysaccharide in human cells and rodent models of peripheral and CNS inflammation. *Brain Behav. Immun.* **2017**, *64*, 285–295. [[CrossRef](#)] [[PubMed](#)]
47. Ricciarelli, R.; Brullo, C.; Prickaerts, J.; Arancio, O.; Villa, C.; Rebosio, C.; Calcagno, E.; Balbi, M.; van Hagen, B.T.; Argyrousi, E.K.; et al. Memory-enhancing effects of GEBR-32a, a new PDE4D inhibitor holding promise for the treatment of Alzheimer's disease. *Sci. Rep.* **2017**, *7*, 46320. [[CrossRef](#)]
48. Zhang, C.; Xu, Y.; Chowdhary, A.; Fox, D., 3rd; Gurney, M.E.; Zhang, H.T.; Auerbach, B.D.; Salvi, R.J.; Yang, M.; Li, G.; et al. Memory enhancing effects of BPN14770, an allosteric inhibitor of phosphodiesterase-4D, in wild-type and humanized mice. *Neuropsychopharmacology* **2018**, *43*, 2299–2309. [[CrossRef](#)]
49. Conti, M.; Beavo, J. Biochemistry and physiology of cyclic nucleotide phosphodiesterases: Essential components in cyclic nucleotide signaling. *Annu. Rev. Biochem.* **2007**, *76*, 481–511. [[CrossRef](#)]
50. Maurice, D.H.; Ke, H.; Ahmad, F.; Wang, Y.; Chung, J.; Manganiello, V.C. Advances in targeting cyclic nucleotide phosphodiesterases. *Nat. Rev. Drug Discov.* **2014**, *13*, 290–314. [[CrossRef](#)]
51. Baillie, G.S.; Tejada, G.S.; Kelly, M.P. Therapeutic targeting of 3',5'-cyclic nucleotide phosphodiesterases: Inhibition and beyond. *Nat. Rev. Drug Discov.* **2019**, *18*, 770–796. [[CrossRef](#)] [[PubMed](#)]
52. Oba, Y.; Lone, N.A. Efficacy and safety of roflumilast in patients with chronic obstructive pulmonary disease: A systematic review and meta-analysis. *Ther. Adv. Respir. Dis.* **2013**, *7*, 13–24. [[CrossRef](#)] [[PubMed](#)]
53. Papp, K.; Cather, J.C.; Rosoph, L.; Sofen, H.; Langley, R.G.; Matheson, R.T.; Hu, C.; Day, R.M. Efficacy of apremilast in the treatment of moderate to severe psoriasis: A randomised controlled trial. *Lancet* **2012**, *380*, 738–746. [[CrossRef](#)]
54. Jarnagin, K.; Chanda, S.; Coronado, D.; Ciaravino, V.; Zane, L.T.; Guttman-Yassky, E.; Lebwohl, M.G. Crisaborole Topical Ointment, 2%: A Nonsteroidal, Topical, Anti-Inflammatory Phosphodiesterase 4 Inhibitor in Clinical Development for the Treatment of Atopic Dermatitis. *J. Drugs Dermatol.* **2016**, *15*, 390–396. [[CrossRef](#)] [[PubMed](#)]
55. Mulhall, A.M.; Droege, C.A.; Ernst, N.E.; Panos, R.J.; Zafar, M.A. Phosphodiesterase 4 inhibitors for the treatment of chronic obstructive pulmonary disease: A review of current and developing drugs. *Expert Opin. Investig. Drugs* **2015**, *24*, 1597–1611. [[CrossRef](#)]

56. Singh, D.; Martinez, F.J.; Watz, H.; Bengtsson, T.; Maurer, B.T. A dose-ranging study of the inhaled dual phosphodiesterase 3 and 4 inhibitor ensifentrine in COPD. *Respir. Res.* **2020**, *21*, 47. [[CrossRef](#)] [[PubMed](#)]
57. Zhang, H.T.; Huang, Y.; Suvarna, N.U.; Deng, C.; Crissman, A.M.; Hopper, A.T.; De Vivo, M.; Rose, G.M.; O'Donnell, J.M. Effects of the novel PDE4 inhibitors MEM1018 and MEM1091 on memory in the radial-arm maze and inhibitory avoidance tests in rats. *Psychopharmacology (Berl)* **2005**, *179*, 613–619. [[CrossRef](#)]
58. Tempesta, D.; Mazza, M.; Serroni, N.; Moschetta, F.S.; Di Giannantonio, M.; Ferrara, M.; De Berardis, D. Neuropsychological functioning in young subjects with generalized anxiety disorder with and without pharmacotherapy. *Prog. Neuro-psychopharmacol. Biol. Psychiatry* **2013**, *45*, 236–241. [[CrossRef](#)]
59. Rock, P.L.; Roiser, J.P.; Riedel, W.J.; Blackwell, A.D. Cognitive impairment in depression: A systematic review and meta-analysis. *Psychol. Med.* **2014**, *44*, 2029–2040. [[CrossRef](#)]
60. Prosdocimi, T.; Mollica, L.; Donini, S.; Semrau, M.S.; Lucarelli, A.P.; Aiolfi, E.; Cavalli, A.; Storici, P.; Alfei, S.; Brullo, C.; et al. Molecular Bases of PDE4D Inhibition by Memory-Enhancing GEBR Library Compounds. *Biochemistry* **2018**, *57*, 2876–2888. [[CrossRef](#)]
61. Cui, S.Y.; Yang, M.X.; Zhang, Y.H.; Zheng, V.; Zhang, H.T.; Gurney, M.E.; Xu, Y.; O'Donnell, J.M. Protection from Amyloid beta Peptide-Induced Memory, Biochemical, and Morphological Deficits by a Phosphodiesterase-4D Allosteric Inhibitor. *J. Pharmacol. Exp. Ther* **2019**, *371*, 250–259. [[CrossRef](#)] [[PubMed](#)]
62. Gurney, M.E.; Nugent, R.A.; Mo, X.; Sindac, J.A.; Hagen, T.J.; Fox, D., 3rd; O'Donnell, J.M.; Zhang, C.; Xu, Y.; Zhang, H.T.; et al. Design and Synthesis of Selective Phosphodiesterase 4D (PDE4D) Allosteric Inhibitors for the Treatment of Fragile X Syndrome and Other Brain Disorders. *J. Med. Chem.* **2019**, *62*, 4884–4901. [[CrossRef](#)] [[PubMed](#)]
63. Titus, D.J.; Wilson, N.M.; Alcazar, O.; Calixte, D.A.; Dietrich, W.D.; Gurney, M.E.; Atkins, C.M. A negative allosteric modulator of PDE4D enhances learning after traumatic brain injury. *Neurobiol. Learn. Mem.* **2018**, *148*, 38–49. [[CrossRef](#)] [[PubMed](#)]
64. Kandel, E.R. The molecular biology of memory storage: A dialogue between genes and synapses. *Science* **2001**, *294*, 1030–1038. [[CrossRef](#)] [[PubMed](#)]
65. Frank, D.A.; Greenberg, M.E. CREB: A mediator of long-term memory from mollusks to mammals. *Cell* **1994**, *79*, 5–8. [[CrossRef](#)]
66. Silva, A.J.; Kogan, J.H.; Frankland, P.W.; Kida, S. CREB and memory. *Annu. Rev. Neurosci.* **1998**, *21*, 127–148. [[CrossRef](#)]
67. Newton, S.S.; Thome, J.; Wallace, T.L.; Shirayama, Y.; Schlesinger, L.; Sakai, N.; Chen, J.; Neve, R.; Nestler, E.J.; Duman, R.S. Inhibition of cAMP response element-binding protein or dynorphin in the nucleus accumbens produces an antidepressant-like effect. *J. Neurosci.* **2002**, *22*, 10883–10890. [[CrossRef](#)]
68. Gloerich, M.; Bos, J.L. Epac: Defining a new mechanism for cAMP action. *Annu. Rev. Pharmacol. Toxicol.* **2010**, *50*, 355–375. [[CrossRef](#)]
69. Schmidt, M.; Dekker, F.J.; Maarsingh, H. Exchange protein directly activated by cAMP (epac): A multidomain cAMP mediator in the regulation of diverse biological functions. *Pharmacol. Rev.* **2013**, *65*, 670–709. [[CrossRef](#)]
70. Kaupp, U.B.; Seifert, R. Cyclic nucleotide-gated ion channels. *Physiol. Rev.* **2002**, *82*, 769–824. [[CrossRef](#)]
71. Schindler, R.F.; Brand, T. The Popeye domain containing protein family—A novel class of cAMP effectors with important functions in multiple tissues. *Prog. Biophys. Mol. Biol.* **2016**, *120*, 28–36. [[CrossRef](#)] [[PubMed](#)]
72. Bolger, G.; Michaeli, T.; Martins, T.; St John, T.; Steiner, B.; Rodgers, L.; Riggs, M.; Wigler, M.; Ferguson, K. A family of human phosphodiesterases homologous to the dunce learning and memory gene product of *Drosophila melanogaster* are potential targets for antidepressant drugs. *Mol. Cell Biol.* **1993**, *13*, 6558–6571. [[CrossRef](#)] [[PubMed](#)]
73. Johnson, K.R.; Nicodemus-Johnson, J.; Danziger, R.S. An evolutionary analysis of cAMP-specific Phosphodiesterase 4 alternative splicing. *BMC Evol. Biol.* **2010**, *10*, 247. [[CrossRef](#)] [[PubMed](#)]
74. Bolger, G.B.; Rodgers, L.; Riggs, M. Differential CNS expression of alternative mRNA isoforms of the mammalian genes encoding cAMP-specific phosphodiesterases. *Gene* **1994**, *149*, 237–244. [[CrossRef](#)]
75. Takahashi, M.; Terwilliger, R.; Lane, C.; Mezes, P.S.; Conti, M.; Duman, R.S. Chronic antidepressant administration increases the expression of cAMP-specific phosphodiesterase 4A and 4B isoforms. *J. Neurosci.* **1999**, *19*, 610–618. [[CrossRef](#)] [[PubMed](#)]
76. Cherry, J.A.; Davis, R.L. Cyclic AMP phosphodiesterases are localized in regions of the mouse brain associated with reinforcement, movement, and affect. *J. Comp. Neurol.* **1999**, *407*, 287–301. [[CrossRef](#)]

77. Miro, X.; Perez-Torres, S.; Puigdomenech, P.; Palacios, J.M.; Mengod, G. Differential distribution of PDE4D splice variant mRNAs in rat brain suggests association with specific pathways and presynaptical localization. *Synapse* **2002**, *45*, 259–269. [[CrossRef](#)]
78. D'Sa, C.; Tolbert, L.M.; Conti, M.; Duman, R.S. Regulation of cAMP-specific phosphodiesterases type 4B and 4D (PDE4) splice variants by cAMP signaling in primary cortical neurons. *J. Neurochem.* **2002**, *81*, 745–757. [[CrossRef](#)]
79. D'Sa, C.; Eisch, A.J.; Bolger, G.B.; Duman, R.S. Differential expression and regulation of the cAMP-selective phosphodiesterase type 4A splice variants in rat brain by chronic antidepressant administration. *Eur. J. Neurosci.* **2005**, *22*, 1463–1475. [[CrossRef](#)]
80. Reyes-Irisarri, E.; Perez-Torres, S.; Miro, X.; Martinez, E.; Puigdomenech, P.; Palacios, J.M.; Mengod, G. Differential distribution of PDE4B splice variant mRNAs in rat brain and the effects of systemic administration of LPS in their expression. *Synapse* **2008**, *62*, 74–79. [[CrossRef](#)]
81. Nishi, A.; Kuroiwa, M.; Miller, D.B.; O'Callaghan, J.P.; Bateup, H.S.; Shuto, T.; Sotogaku, N.; Fukuda, T.; Heintz, N.; Greengard, P.; et al. Distinct roles of PDE4 and PDE10A in the regulation of cAMP/PKA signaling in the striatum. *J. Neurosci.* **2008**, *28*, 10460–10471. [[CrossRef](#)] [[PubMed](#)]
82. Mori, F.; Perez-Torres, S.; De Caro, R.; Porzionato, A.; Macchi, V.; Beleta, J.; Gavalda, A.; Palacios, J.M.; Mengod, G. The human area postrema and other nuclei related to the emetic reflex express cAMP phosphodiesterases 4B and 4D. *J. Chem. Neuroanat.* **2010**, *40*, 36–42. [[CrossRef](#)] [[PubMed](#)]
83. Kuroiwa, M.; Snyder, G.L.; Shuto, T.; Fukuda, A.; Yanagawa, Y.; Benavides, D.R.; Nairn, A.C.; Bibb, J.A.; Greengard, P.; Nishi, A. Phosphodiesterase 4 inhibition enhances the dopamine D1 receptor/PKA/DARPP-32 signaling cascade in frontal cortex. *Psychopharmacology (Berl)* **2012**, *219*, 1065–1079. [[CrossRef](#)] [[PubMed](#)]
84. Ahmed, T.; Frey, J.U. Expression of the specific type IV phosphodiesterase gene PDE4B3 during different phases of long-term potentiation in single hippocampal slices of rats in vitro. *Neuroscience* **2003**, *117*, 627–638. [[CrossRef](#)]
85. Zhang, K.Y.; Card, G.L.; Suzuki, Y.; Artis, D.R.; Fong, D.; Gillette, S.; Hsieh, D.; Neiman, J.; West, B.L.; Zhang, C.; et al. A glutamine switch mechanism for nucleotide selectivity by phosphodiesterases. *Mol. Cell* **2004**, *15*, 279–286. [[CrossRef](#)] [[PubMed](#)]
86. Burgin, A.B.; Magnusson, O.T.; Singh, J.; Witte, P.; Staker, B.L.; Bjornsson, J.M.; Thorsteinsdottir, M.; Hrafnisdottir, S.; Hagen, T.; Kiselyov, A.S.; et al. Design of phosphodiesterase 4D (PDE4D) allosteric modulators for enhancing cognition with improved safety. *Nat. Biotechnol.* **2010**, *28*, 63–70. [[CrossRef](#)]
87. Francis, S.H.; Blount, M.A.; Corbin, J.D. Mammalian cyclic nucleotide phosphodiesterases: Molecular mechanisms and physiological functions. *Physiol. Rev.* **2011**, *91*, 651–690. [[CrossRef](#)]
88. Bolger, G.B.; Erdogan, S.; Jones, R.E.; Loughney, K.; Scotland, G.; Hoffmann, R.; Wilkinson, I.; Farrell, C.; Houslay, M.D. Characterization of five different proteins produced by alternatively spliced mRNAs from the human cAMP-specific phosphodiesterase PDE4D gene. *Biochem. J.* **1997**, *328*, 539–548. [[CrossRef](#)]
89. Lamontagne, S.; Meadows, E.; Luk, P.; Normandin, D.; Muise, E.; Boulet, L.; Pon, D.J.; Robichaud, A.; Robertson, G.S.; Metters, K.M.; et al. Localization of phosphodiesterase-4 isoforms in the medulla and nodose ganglion of the squirrel monkey. *Brain Res.* **2001**, *920*, 84–96. [[CrossRef](#)]
90. Whitaker, C.M.; Cooper, N.G. The novel distribution of phosphodiesterase-4 subtypes within the rat retina. *Neuroscience* **2009**, *163*, 1277–1291. [[CrossRef](#)]
91. Lakics, V.; Karran, E.H.; Boess, F.G. Quantitative comparison of phosphodiesterase mRNA distribution in human brain and peripheral tissues. *Neuropharmacology* **2010**, *59*, 367–374. [[CrossRef](#)] [[PubMed](#)]
92. Johansson, E.M.; Reyes-Irisarri, E.; Mengod, G. Comparison of cAMP-specific phosphodiesterase mRNAs distribution in mouse and rat brain. *Neurosci. Lett.* **2012**, *525*, 1–6. [[CrossRef](#)] [[PubMed](#)]
93. Oliva, A.A., Jr.; Kang, Y.; Furonos, C.; Alonso, O.F.; Bruno, O.; Dietrich, W.D.; Atkins, C.M. Phosphodiesterase isoform-specific expression induced by traumatic brain injury. *J. Neurochem.* **2012**, *123*, 1019–1029. [[CrossRef](#)] [[PubMed](#)]
94. Kelly, M.P.; Adamowicz, W.; Bove, S.; Hartman, A.J.; Mariga, A.; Pathak, G.; Reinhart, V.; Romegialli, A.; Kleiman, R.J. Select 3', 5'-cyclic nucleotide phosphodiesterases exhibit altered expression in the aged rodent brain. *Cell Signal.* **2014**, *26*, 383–397. [[CrossRef](#)] [[PubMed](#)]
95. Kelly, M.P. Cyclic nucleotide signaling changes associated with normal aging and age-related diseases of the brain. *Cell Signal.* **2018**, *42*, 281–291. [[CrossRef](#)] [[PubMed](#)]

96. Gretarsdottir, S.; Thorleifsson, G.; Reynisdottir, S.T.; Manolescu, A.; Jonsdottir, S.; Jonsdottir, T.; Gudmundsdottir, T.; Bjarnadottir, S.M.; Einarsson, O.B.; Gudjonsdottir, H.M.; et al. The gene encoding phosphodiesterase 4D confers risk of ischemic stroke. *Nat. Genet.* **2003**, *35*, 131–138. [[CrossRef](#)] [[PubMed](#)]
97. Wang, D.; Deng, C.; Bugaj-Gaweda, B.; Kwan, M.; Gunwaldsen, C.; Leonard, C.; Xin, X.; Hu, Y.; Unterbeck, A.; De Vivo, M. Cloning and characterization of novel PDE4D isoforms PDE4D6 and PDE4D7. *Cell Signal.* **2003**, *15*, 883–891. [[CrossRef](#)]
98. Richter, W.; Jin, S.L.; Conti, M. Splice variants of the cyclic nucleotide phosphodiesterase PDE4D are differentially expressed and regulated in rat tissue. *Biochem. J.* **2005**, *388*, 803–811. [[CrossRef](#)]
99. Chandrasekaran, A.; Toh, K.Y.; Low, S.H.; Tay, S.K.; Brenner, S.; Goh, D.L. Identification and characterization of novel mouse PDE4D isoforms: Molecular cloning, subcellular distribution and detection of isoform-specific intracellular localization signals. *Cell Signal.* **2008**, *20*, 139–153. [[CrossRef](#)]
100. Lynex, C.N.; Li, Z.; Chen, M.L.; Toh, K.Y.; Low, R.W.; Goh, D.L.; Tay, S.K. Identification and molecular characterization of a novel PDE4D11 cAMP-specific phosphodiesterase isoform. *Cell Signal.* **2008**, *20*, 2247–2255. [[CrossRef](#)]
101. Yarwood, S.J.; Steele, M.R.; Scotland, G.; Houslay, M.D.; Bolger, G.B. The RACK1 signaling scaffold protein selectively interacts with the cAMP-specific phosphodiesterase PDE4D5 isoform. *J. Biol. Chem.* **1999**, *274*, 14909–14917. [[CrossRef](#)] [[PubMed](#)]
102. Bolger, G.B.; McCahill, A.; Yarwood, S.J.; Steele, M.S.; Warwicker, J.; Houslay, M.D. Delineation of RAID1, the RACK1 interaction domain located within the unique N-terminal region of the cAMP-specific phosphodiesterase, PDE4D5. *BMC Biochem.* **2002**, *3*, 24. [[CrossRef](#)] [[PubMed](#)]
103. Bolger, G.B.; Baillie, G.S.; Li, X.; Lynch, M.J.; Herzyk, P.; Mohamed, A.; Mitchell, L.H.; McCahill, A.; Hundsrucker, C.; Klussmann, E.; et al. Scanning peptide array analyses identify overlapping binding sites for the signalling scaffold proteins, beta-arrestin and RACK1, in cAMP-specific phosphodiesterase PDE4D5. *Biochem. J.* **2006**, *398*, 23–36. [[CrossRef](#)] [[PubMed](#)]
104. Steele, M.R.; McCahill, A.; Thompson, D.S.; MacKenzie, C.; Isaacs, N.W.; Houslay, M.D.; Bolger, G.B. Identification of a surface on the beta-propeller protein RACK1 that interacts with the cAMP-specific phosphodiesterase PDE4D5. *Cell Signal.* **2001**, *13*, 507–513. [[CrossRef](#)]
105. Baillie, G.S.; Adams, D.R.; Bhari, N.; Houslay, T.M.; Vadrevu, S.; Meng, D.; Li, X.; Dunlop, A.; Milligan, G.; Bolger, G.B.; et al. Mapping binding sites for the PDE4D5 cAMP-specific phosphodiesterase to the N- and C-domains of beta-arrestin using spot-immobilized peptide arrays. *Biochem. J.* **2007**, *404*, 71–80. [[CrossRef](#)] [[PubMed](#)]
106. Smith, K.J.; Baillie, G.S.; Hyde, E.I.; Li, X.; Houslay, T.M.; McCahill, A.; Dunlop, A.J.; Bolger, G.B.; Klussmann, E.; Adams, D.R.; et al. 1H NMR structural and functional characterisation of a cAMP-specific phosphodiesterase-4D5 (PDE4D5) N-terminal region peptide that disrupts PDE4D5 interaction with the signalling scaffold proteins, beta-arrestin and RACK1. *Cell Signal.* **2007**, *19*, 2612–2624. [[CrossRef](#)]
107. Bolger, G.B. RACK1 and beta-arrestin2 attenuate dimerization of PDE4 cAMP phosphodiesterase PDE4D5. *Cell Signal.* **2016**, *28*, 706–712. [[CrossRef](#)]
108. Perry, S.J.; Baillie, G.S.; Kohout, T.A.; McPhee, I.; Magiera, M.M.; Ang, K.L.; Miller, W.E.; McLean, A.J.; Conti, M.; Houslay, M.D.; et al. Targeting of cyclic AMP degradation to beta 2-adrenergic receptors by beta-arrestins. *Science* **2002**, *298*, 834–836. [[CrossRef](#)]
109. Baillie, G.S.; Sood, A.; McPhee, I.; Gall, I.; Perry, S.J.; Lefkowitz, R.J.; Houslay, M.D. β -Arrestin-mediated PDE4 cAMP phosphodiesterase recruitment regulates beta-adrenoceptor switching from Gs to Gi. *Proc. Natl. Acad. Sci. USA* **2003**, *100*, 940–945. [[CrossRef](#)]
110. Bolger, G.B.; McCahill, A.; Huston, E.; Cheung, Y.F.; McSorley, T.; Baillie, G.S.; Houslay, M.D. The unique amino-terminal region of the PDE4D5 cAMP phosphodiesterase isoform confers preferential interaction with beta-arrestins. *J. Biol. Chem.* **2003**, *278*, 49230–49238. [[CrossRef](#)]
111. Lynch, M.J.; Baillie, G.S.; Mohamed, A.; Li, X.; Maisonneuve, C.; Klussmann, E.; Van Heeke, G.; Houslay, M.D. RNA Silencing Identifies PDE4D5 as the Functionally Relevant cAMP Phosphodiesterase Interacting with β Arrestin to Control the Protein Kinase A/AKAP79-mediated Switching of the β 2-Adrenergic Receptor to Activation of ERK in HEK293B2 Cells. *J. Biol. Chem.* **2005**, *280*, 33178–33189. [[CrossRef](#)] [[PubMed](#)]

112. Richter, W.; Day, P.; Agrawal, R.; Bruss, M.D.; Granier, S.; Wang, Y.L.; Rasmussen, S.G.; Horner, K.; Wang, P.; Lei, T.; et al. Signaling from beta1- and beta2-adrenergic receptors is defined by differential interactions with PDE4. *EMBO J.* **2008**, *27*, 384–393. [[CrossRef](#)] [[PubMed](#)]
113. Bradaia, A.; Berton, F.; Ferrari, S.; Luscher, C. beta-Arrestin2, interacting with phosphodiesterase 4, regulates synaptic release probability and presynaptic inhibition by opioids. *Proc. Natl. Acad. Sci. USA* **2005**, *102*, 3034–3039. [[CrossRef](#)] [[PubMed](#)]
114. Li, X.; Huston, E.; Lynch, M.J.; Houslay, M.D.; Baillie, G.S. Phosphodiesterase-4 influences the PKA phosphorylation status and membrane translocation of G-protein receptor kinase 2 (GRK2) in HEK-293beta2 cells and cardiac myocytes. *Biochem. J.* **2006**, *394*, 427–435. [[CrossRef](#)] [[PubMed](#)]
115. Hoffmann, R.; Baillie, G.S.; MacKenzie, S.J.; Yarwood, S.J.; Houslay, M.D. The MAP kinase ERK2 inhibits the cyclic AMP-specific phosphodiesterase HSPDE4D3 by phosphorylating it at Ser579. *EMBO J.* **1999**, *18*, 893–903. [[CrossRef](#)]
116. MacKenzie, S.J.; Baillie, G.S.; McPhee, I.; Bolger, G.B.; Houslay, M.D. ERK2 mitogen-activated protein kinase binding, phosphorylation, and regulation of the PDE4D cAMP-specific phosphodiesterases. The involvement of COOH-terminal docking sites and NH2-terminal UCR regions. *J. Biol. Chem.* **2000**, *275*, 16609–16617. [[CrossRef](#)]
117. Song, R.S.; Massenburg, B.; Wenderski, W.; Jayaraman, V.; Thompson, L.; Neves, S.R. ERK regulation of phosphodiesterase 4 enhances dopamine-stimulated AMPA receptor membrane insertion. *Proc. Natl. Acad. Sci. USA* **2013**, *110*, 15437–15442. [[CrossRef](#)]
118. Mackenzie, K.F.; Wallace, D.A.; Hill, E.V.; Anthony, D.F.; Henderson, D.J.; Houslay, D.M.; Arthur, J.S.; Baillie, G.S.; Houslay, M.D. Phosphorylation of cAMP-specific PDE4A5 (phosphodiesterase-4A5) by MK2 (MAPKAPK2) attenuates its activation through protein kinase A phosphorylation. *Biochem. J.* **2011**, *435*, 755–769. [[CrossRef](#)]
119. Houslay, K.F.; Christian, F.; MacLeod, R.; Adams, D.R.; Houslay, M.D.; Baillie, G.S. Identification of a multifunctional docking site on the catalytic unit of phosphodiesterase-4 (PDE4) that is utilised by multiple interaction partners. *Biochem. J.* **2017**, *474*, 597–609. [[CrossRef](#)]
120. Sette, C.; Conti, M. Phosphorylation and activation of a cAMP-specific phosphodiesterase by the cAMP-dependent protein kinase. Involvement of serine 54 in the enzyme activation. *J. Biol. Chem.* **1996**, *271*, 16526–16534. [[CrossRef](#)]
121. Hoffmann, R.; Wilkinson, I.R.; McCallum, J.F.; Engels, P.; Houslay, M.D. cAMP-specific phosphodiesterase HSPDE4D3 mutants which mimic activation and changes in rolipram inhibition triggered by protein kinase A phosphorylation of Ser-54: Generation of a molecular model. *Biochem. J.* **1998**, *333*, 139–149. [[CrossRef](#)] [[PubMed](#)]
122. Oki, N.; Takahashi, S.I.; Hidaka, H.; Conti, M. Short term feedback regulation of cAMP in FRTL-5 thyroid cells. Role of PDE4D3 phosphodiesterase activation. *J. Biol. Chem.* **2000**, *275*, 10831–10837. [[CrossRef](#)] [[PubMed](#)]
123. MacKenzie, S.J.; Baillie, G.S.; McPhee, I.; MacKenzie, C.; Seamons, R.; McSorley, T.; Millen, J.; Beard, M.B.; Van Heeke, G.; Houslay, M.D. Long PDE4 cAMP specific phosphodiesterases are activated by protein kinase A-mediated phosphorylation of a single serine residue in Upstream Conserved Region 1 (UCR1). *Br. J. Pharmacol.* **2002**, *136*, 421–433. [[CrossRef](#)] [[PubMed](#)]
124. Hill, E.V.; Sheppard, C.L.; Cheung, Y.F.; Gall, I.; Krause, E.; Houslay, M.D. Oxidative stress employs phosphatidyl inositol 3-kinase and ERK signalling pathways to activate cAMP phosphodiesterase-4D3 (PDE4D3) through multi-site phosphorylation at Ser239 and Ser579. *Cell Signal.* **2006**, *18*, 2056–2069. [[CrossRef](#)] [[PubMed](#)]
125. Xu, R.X.; Hassell, A.M.; Vanderwall, D.; Lambert, M.H.; Holmes, W.D.; Luther, M.A.; Rocque, W.J.; Milburn, M.V.; Zhao, Y.; Ke, H.; et al. Atomic structure of PDE4: Insights into phosphodiesterase mechanism and specificity. *Science* **2000**, *288*, 1822–1825. [[CrossRef](#)] [[PubMed](#)]
126. Wang, H.; Peng, M.S.; Chen, Y.; Geng, J.; Robinson, H.; Houslay, M.D.; Cai, J.; Ke, H. Structures of the four subfamilies of phosphodiesterase-4 provide insight into the selectivity of their inhibitors. *Biochem. J.* **2007**, *408*, 193–201. [[CrossRef](#)]
127. Cedervall, P.; Aulabaugh, A.; Geoghegan, K.F.; McLellan, T.J.; Pandit, J. Engineered stabilization and structural analysis of the autoinhibited conformation of PDE4. *Proc. Natl. Acad. Sci. USA* **2015**, *112*, E1414–E1422. [[CrossRef](#)]

128. Bolger, G.B.; Dunlop, A.J.; Meng, D.; Day, J.P.; Klusmann, E.; Baillie, G.S.; Adams, D.R.; Houslay, M.D. Dimerization of cAMP phosphodiesterase-4 (PDE4) in living cells requires interfaces located in both the UCR1 and catalytic unit domains. *Cell Signal.* **2015**, *27*, 756–769. [[CrossRef](#)]
129. Richter, W.; Conti, M. Dimerization of the type 4 cAMP-specific phosphodiesterases is mediated by the upstream conserved regions (UCRs). *J. Biol. Chem.* **2002**, *277*, 40212–40221. [[CrossRef](#)]
130. Richter, W.; Conti, M. The oligomerization state determines regulatory properties and inhibitor sensitivity of type 4 cAMP-specific phosphodiesterases. *J. Biol. Chem.* **2004**, *279*, 30338–30348. [[CrossRef](#)]
131. Xie, M.; Blackman, B.; Scheitrum, C.; Mika, D.; Blanchard, E.; Lei, T.; Conti, M.; Richter, W. The upstream conserved regions (UCRs) mediate homo- and hetero-oligomerization of type 4 cyclic nucleotide phosphodiesterases (PDE4s). *Biochem. J.* **2014**, *459*, 539–550. [[CrossRef](#)] [[PubMed](#)]
132. Blanchard, E.; Zlock, L.; Lao, A.; Mika, D.; Namkung, W.; Xie, M.; Scheitrum, C.; Gruenert, D.C.; Verkman, A.S.; Finkbeiner, W.E.; et al. Anchored PDE4 regulates chloride conductance in wild-type and DeltaF508-CFTR human airway epithelia. *FASEB J.* **2014**, *28*, 791–801. [[CrossRef](#)] [[PubMed](#)]
133. Campbell, S.L.; van Groen, T.; Kadish, I.; Smoot, L.H.M.; Bolger, G.B. Altered phosphorylation, electrophysiology, and behavior on attenuation of PDE4B action in hippocampus. *BMC Neurosci.* **2017**, *18*, 77. [[CrossRef](#)] [[PubMed](#)]
134. McGirr, A.; Lipina, T.V.; Mun, H.S.; Georgiou, J.; Al-Amri, A.H.; Ng, E.; Zhai, D.; Elliott, C.; Cameron, R.T.; Mullins, J.G.; et al. Specific Inhibition of Phosphodiesterase-4B Results in Anxiolysis and Facilitates Memory Acquisition. *Neuropsychopharmacology* **2016**, *41*, 1080–1092. [[CrossRef](#)] [[PubMed](#)]
135. Havekes, R.; Park, A.J.; Tolentino, R.E.; Bruinenberg, V.M.; Tudor, J.C.; Lee, Y.; Hansen, R.T.; Guercio, L.A.; Linton, E.; Neves-Zaph, S.R.; et al. Compartmentalized PDE4A5 Signaling Impairs Hippocampal Synaptic Plasticity and Long-Term Memory. *J. Neurosci.* **2016**, *36*, 8936–8946. [[CrossRef](#)]
136. Havekes, R.; Park, A.J.; Tudor, J.C.; Luczak, V.G.; Hansen, R.T.; Ferri, S.L.; Bruinenberg, V.M.; Poplawski, S.G.; Day, J.P.; Aton, S.J.; et al. Sleep deprivation causes memory deficits by negatively impacting neuronal connectivity in hippocampal area CA1. *Elife* **2016**, *5*. [[CrossRef](#)]
137. Zhang, H.T.; Huang, Y.; Jin, S.L.; Frith, S.A.; Suvarna, N.; Conti, M.; O'Donnell, J.M. Antidepressant-like profile and reduced sensitivity to rolipram in mice deficient in the PDE4D phosphodiesterase enzyme. *Neuropsychopharmacology* **2002**, *27*, 587–595. [[CrossRef](#)]
138. Siuciak, J.A.; Chapin, D.S.; McCarthy, S.A.; Martin, A.N. Antipsychotic profile of rolipram: Efficacy in rats and reduced sensitivity in mice deficient in the phosphodiesterase-4B (PDE4B) enzyme. *Psychopharmacology (Berl)* **2007**, *192*, 415–424. [[CrossRef](#)]
139. Siuciak, J.A.; McCarthy, S.A.; Chapin, D.S.; Martin, A.N. Behavioral and neurochemical characterization of mice deficient in the phosphodiesterase-4B (PDE4B) enzyme. *Psychopharmacology (Berl)* **2008**, *197*, 115–126. [[CrossRef](#)]
140. Zhang, H.T.; Huang, Y.; Masood, A.; Stolinski, L.R.; Li, Y.; Zhang, L.; Dlaboga, D.; Jin, S.L.; Conti, M.; O'Donnell, J.M. Anxiogenic-like behavioral phenotype of mice deficient in phosphodiesterase 4B (PDE4B). *Neuropsychopharmacology* **2008**, *33*, 1611–1623. [[CrossRef](#)]
141. Rutten, K.; Wallace, T.L.; Works, M.; Prickaerts, J.; Blokland, A.; Novak, T.J.; Santarelli, L.; Misner, D.L. Enhanced long-term depression and impaired reversal learning in phosphodiesterase 4B-knockout (PDE4B^{-/-}) mice. *Neuropharmacology* **2011**, *61*, 138–147. [[CrossRef](#)] [[PubMed](#)]
142. Li, Y.F.; Cheng, Y.F.; Huang, Y.; Conti, M.; Wilson, S.P.; O'Donnell, J.M.; Zhang, H.T. Phosphodiesterase-4D knock-out and RNA interference-mediated knock-down enhance memory and increase hippocampal neurogenesis via increased cAMP signaling. *J. Neurosci.* **2011**, *31*, 172–183. [[CrossRef](#)] [[PubMed](#)]
143. Hansen, R.T., III; Conti, M.; Zhang, H.T. Mice deficient in phosphodiesterase-4A display anxiogenic-like behavior. *Psychopharmacology (Berl)* **2014**, *231*, 2941–2954. [[CrossRef](#)] [[PubMed](#)]
144. Schaefer, T.L.; Braun, A.A.; Amos-Kroohs, R.M.; Williams, M.T.; Ostertag, E.; Vorhees, C.V. A new model of Pde4d deficiency: Genetic knock-down of PDE4D enzyme in rats produces an antidepressant phenotype without spatial cognitive effects. *Genes Brain Behav.* **2012**, *11*, 614–622. [[CrossRef](#)] [[PubMed](#)]
145. Wang, Z.Z.; Zhang, Y.; Liu, Y.Q.; Zhao, N.; Zhang, Y.Z.; Yuan, L.; An, L.; Li, J.; Wang, X.Y.; Qin, J.J.; et al. RNA interference-mediated phosphodiesterase 4D splice variants knock-down in the prefrontal cortex produces antidepressant-like and cognition-enhancing effects. *Br. J. Pharmacol.* **2013**, *168*, 1001–1014. [[CrossRef](#)] [[PubMed](#)]

146. Wang, Z.Z.; Yang, W.X.; Zhang, Y.; Zhao, N.; Zhang, Y.Z.; Liu, Y.Q.; Xu, Y.; Wilson, S.P.; O'Donnell, J.M.; Zhang, H.T.; et al. Phosphodiesterase-4D Knock-down in the Prefrontal Cortex Alleviates Chronic Unpredictable Stress-Induced Depressive-Like Behaviors and Memory Deficits in Mice. *Sci. Rep.* **2015**, *5*, 11332. [[CrossRef](#)] [[PubMed](#)]
147. Zhang, C.; Cheng, Y.; Wang, H.; Wang, C.; Wilson, S.P.; Xu, J.; Zhang, H.T. RNA interference-mediated knockdown of long-form phosphodiesterase-4D (PDE4D) enzyme reverses amyloid-beta42-induced memory deficits in mice. *J. Alzheimers. Dis.* **2014**, *38*, 269–280. [[CrossRef](#)]
148. Xiang, Y.; Naro, F.; Zoudilova, M.; Jin, S.L.; Conti, M.; Kobilka, B. Phosphodiesterase 4D is required for beta2 adrenoceptor subtype-specific signaling in cardiac myocytes. *Proc. Natl. Acad. Sci. USA* **2005**, *102*, 909–914. [[CrossRef](#)]
149. Nino, G.; Hu, A.; Grunstein, J.S.; Grunstein, M.M. Mechanism regulating proasthmatic effects of prolonged homologous beta2-adrenergic receptor desensitization in airway smooth muscle. *Am. J. Physiol. Lung Cell Mol. Physiol.* **2009**, *297*, L746–L757. [[CrossRef](#)]
150. Hu, A.; Nino, G.; Grunstein, J.S.; Fatma, S.; Grunstein, M.M. Prolonged heterologous beta2-adrenoceptor desensitization promotes proasthmatic airway smooth muscle function via PKA/ERK1/2-mediated phosphodiesterase-4 induction. *Am. J. Physiol. Lung Cell Mol. Physiol.* **2008**, *294*, L1055–L1067. [[CrossRef](#)]
151. Billington, C.K.; Le Jeune, I.R.; Young, K.W.; Hall, I.P. A major functional role for phosphodiesterase 4D5 in human airway smooth muscle cells. *Am. J. Respir. Cell Mol. Biol.* **2008**, *38*, 1–7. [[CrossRef](#)] [[PubMed](#)]
152. Niimi, K.; Ge, Q.; Moir, L.M.; Ammit, A.J.; Trian, T.; Burgess, J.K.; Black, J.L.; Oliver, B.G. β 2-Agonists upregulate PDE4 mRNA but not protein or activity in human airway smooth muscle cells from asthmatic and nonasthmatic volunteers. *Am. J. Physiol. Lung Cell Mol. Physiol.* **2012**, *302*, L334–L342. [[CrossRef](#)] [[PubMed](#)]
153. Serrels, B.; Sandilands, E.; Serrels, A.; Baillie, G.; Houslay, M.D.; Brunton, V.G.; Canel, M.; Machesky, L.M.; Anderson, K.I.; Frame, M.C. A complex between FAK, RACK1, and PDE4D5 controls spreading initiation and cancer cell polarity. *Curr. Biol.* **2010**, *20*, 1086–1092. [[CrossRef](#)] [[PubMed](#)]
154. Yun, S.; Budatha, M.; Dahlman, J.E.; Coon, B.G.; Cameron, R.T.; Langer, R.; Anderson, D.G.; Baillie, G.; Schwartz, M.A. Interaction between integrin alpha5 and PDE4D regulates endothelial inflammatory signalling. *Nat. Cell Biol.* **2016**, *18*, 1043–1053. [[CrossRef](#)] [[PubMed](#)]
155. Mayford, M.; Baranes, D.; Podsypanina, K.; Kandel, E.R. The 3'-untranslated region of CaMKII alpha is a cis-acting signal for the localization and translation of mRNA in dendrites. *Proc. Natl. Acad. Sci. USA* **1996**, *93*, 13250–13255. [[CrossRef](#)] [[PubMed](#)]
156. Mayford, M.; Bach, M.E.; Huang, Y.Y.; Wang, L.; Hawkins, R.D.; Kandel, E.R. Control of memory formation through regulated expression of a CaMKII transgene. *Science* **1996**, *274*, 1678–1683. [[CrossRef](#)] [[PubMed](#)]
157. Tsien, J.Z.; Chen, D.F.; Gerber, D.; Tom, C.; Mercer, E.H.; Anderson, D.J.; Mayford, M.; Kandel, E.R.; Tonegawa, S. Subregion- and cell type-restricted gene knockout in mouse brain. *Cell* **1996**, *87*, 1317–1326. [[CrossRef](#)]
158. Hatcher, J.P.; Jones, D.N.; Rogers, D.C.; Hatcher, P.D.; Reavill, C.; Hagan, J.J.; Hunter, A.J. Development of SHIRPA to characterise the phenotype of gene-targeted mice. *Behav. Brain Res.* **2001**, *125*, 43–47. [[CrossRef](#)]
159. Rogers, D.C.; Fisher, E.M.; Brown, S.D.; Peters, J.; Hunter, A.J.; Martin, J.E. Behavioral and functional analysis of mouse phenotype: SHIRPA, a proposed protocol for comprehensive phenotype assessment. *Mamm. Genome* **1997**, *8*, 711–713. [[CrossRef](#)]
160. Millar, J.K.; Pickard, B.S.; Mackie, S.; James, R.; Christie, S.; Buchanan, S.R.; Malloy, M.P.; Chubb, J.E.; Huston, E.; Baillie, G.S.; et al. DISC1 and PDE4B are interacting genetic factors in schizophrenia that regulate cAMP signaling. *Science* **2005**, *310*, 1187–1191. [[CrossRef](#)]
161. Bradshaw, N.J.; Soares, D.C.; Carlyle, B.C.; Ogawa, F.; Davidson-Smith, H.; Christie, S.; Mackie, S.; Thomson, P.A.; Porteous, D.J.; Millar, J.K. PKA phosphorylation of NDE1 is DISC1/PDE4 dependent and modulates its interaction with LIS1 and NDEL1. *J. Neurosci.* **2011**, *31*, 9043–9054. [[CrossRef](#)] [[PubMed](#)]
162. Murdoch, H.; Mackie, S.; Collins, D.M.; Hill, E.V.; Bolger, G.B.; Klussmann, E.; Porteous, D.J.; Millar, J.K.; Houslay, M.D. Isoform-selective susceptibility of DISC1/phosphodiesterase-4 complexes to dissociation by elevated intracellular cAMP levels. *J. Neurosci.* **2007**, *27*, 9513–9524. [[CrossRef](#)] [[PubMed](#)]
163. Bradshaw, N.J.; Ogawa, F.; Antolin-Fontes, B.; Chubb, J.E.; Carlyle, B.C.; Christie, S.; Claessens, A.; Porteous, D.J.; Millar, J.K. DISC1, PDE4B, and NDE1 at the centrosome and synapse. *Biochem. Biophys. Res. Commun.* **2008**, *377*, 1091–1096. [[CrossRef](#)] [[PubMed](#)]

164. Soda, T.; Frank, C.; Ishizuka, K.; Baccarella, A.; Park, Y.U.; Flood, Z.; Park, S.K.; Sawa, A.; Tsai, L.H. DISC1-ATF4 transcriptional repression complex: Dual regulation of the cAMP-PDE4 cascade by DISC1. *Mol. Psychiatry* **2013**, *18*, 898–908. [[CrossRef](#)]
165. Clapcote, S.J.; Lipina, T.V.; Millar, J.K.; Mackie, S.; Christie, S.; Ogawa, F.; Lerch, J.P.; Trimble, K.; Uchiyama, M.; Sakuraba, Y.; et al. Behavioral phenotypes of Disc1 missense mutations in mice. *Neuron* **2007**, *54*, 387–402. [[CrossRef](#)]
166. Lipina, T.V.; Wang, M.; Liu, F.; Roder, J.C. Synergistic interactions between PDE4B and GSK-3: DISC1 mutant mice. *Neuropharmacology* **2012**, *62*, 1252–1262. [[CrossRef](#)]
167. Selcher, J.C.; Nekrasova, T.; Paylor, R.; Landreth, G.E.; Sweatt, J.D. Mice lacking the ERK1 isoform of MAP kinase are unimpaired in emotional learning. *Learn. Mem.* **2001**, *8*, 11–19. [[CrossRef](#)]
168. Bourtchuladze, R.; Frenguelli, B.; Blendy, J.; Cioffi, D.; Schutz, G.; Silva, A.J. Deficient long-term memory in mice with a targeted mutation of the cAMP-responsive element-binding protein. *Cell* **1994**, *79*, 59–68. [[CrossRef](#)]
169. Kida, S.; Josselyn, S.A.; de Ortiz, S.P.; Kogan, J.H.; Chevere, I.; Masushige, S.; Silva, A.J. CREB required for the stability of new and reactivated fear memories. *Nat. Neurosci.* **2002**, *5*, 348–355. [[CrossRef](#)]
170. Barco, A.; Alarcon, J.M.; Kandel, E.R. Expression of constitutively active CREB protein facilitates the late phase of long-term potentiation by enhancing synaptic capture. *Cell* **2002**, *108*, 689–703. [[CrossRef](#)]
171. Pittenger, C.; Huang, Y.Y.; Paletzki, R.F.; Bourtchouladze, R.; Scanlin, H.; Vronskaya, S.; Kandel, E.R. Reversible inhibition of CREB/ATF transcription factors in region CA1 of the dorsal hippocampus disrupts hippocampus-dependent spatial memory. *Neuron* **2002**, *34*, 447–462. [[CrossRef](#)]
172. Kogan, J.H.; Frankland, P.W.; Blendy, J.A.; Coblenz, J.; Marowitz, Z.; Schutz, G.; Silva, A.J. Spaced training induces normal long-term memory in CREB mutant mice. *Curr. Biol.* **1997**, *7*, 1–11. [[CrossRef](#)]
173. Wu, Z.L.; Thomas, S.A.; Villacres, E.C.; Xia, Z.; Simmons, M.L.; Chavkin, C.; Palmiter, R.D.; Storm, D.R. Altered behavior and long-term potentiation in type I adenylyl cyclase mutant mice. *Proc. Natl. Acad. Sci. USA* **1995**, *92*, 220–224. [[CrossRef](#)] [[PubMed](#)]
174. Yang, Y.; Shu, X.; Liu, D.; Shang, Y.; Wu, Y.; Pei, L.; Xu, X.; Tian, Q.; Zhang, J.; Qian, K.; et al. EPAC null mutation impairs learning and social interactions via aberrant regulation of miR-124 and Zif268 translation. *Neuron* **2012**, *73*, 774–788. [[CrossRef](#)] [[PubMed](#)]
175. Srivastava, D.P.; Jones, K.A.; Woolfrey, K.M.; Burgdorf, J.; Russell, T.A.; Kalmbach, A.; Lee, H.; Yang, C.; Bradberry, M.M.; Wokosin, D.; et al. Social, communication, and cortical structural impairments in Epac2-deficient mice. *J. Neurosci.* **2012**, *32*, 11864–11878. [[CrossRef](#)] [[PubMed](#)]
176. Morris, R.G.; Garrud, P.; Rawlins, J.N.; O'Keefe, J. Place navigation impaired in rats with hippocampal lesions. *Nature* **1982**, *297*, 681–683. [[CrossRef](#)]
177. Abel, T.; Nguyen, P.V.; Barad, M.; Deuel, T.A.; Kandel, E.R.; Bourtchouladze, R. Genetic demonstration of a role for PKA in the late phase of LTP and in hippocampus-based long-term memory. *Cell* **1997**, *88*, 615–626. [[CrossRef](#)]
178. Pittenger, C.; Fasano, S.; Mazzocchi-Jones, D.; Dunnett, S.B.; Kandel, E.R.; Brambilla, R. Impaired bidirectional synaptic plasticity and procedural memory formation in striatum-specific cAMP response element-binding protein-deficient mice. *J. Neurosci.* **2006**, *26*, 2808–2813. [[CrossRef](#)]
179. Ahn, S.; Ginty, D.D.; Linden, D.J. A late phase of cerebellar long-term depression requires activation of CaMKIV and CREB. *Neuron* **1999**, *23*, 559–568. [[CrossRef](#)]
180. Lonze, B.E.; Riccio, A.; Cohen, S.; Ginty, D.D. Apoptosis, axonal growth defects, and degeneration of peripheral neurons in mice lacking CREB. *Neuron* **2002**, *34*, 371–385. [[CrossRef](#)]
181. Burgin, K.E.; Waxham, M.N.; Rickling, S.; Westgate, S.A.; Mobley, W.C.; Kelly, P.T. In situ hybridization histochemistry of Ca²⁺/calmodulin-dependent protein kinase in developing rat brain. *J. Neurosci.* **1990**, *10*, 1788–1798. [[CrossRef](#)] [[PubMed](#)]
182. Mayford, M.; Wang, J.; Kandel, E.R.; O'Dell, T.J. CaMKII regulates the frequency-response function of hippocampal synapses for the production of both LTD and LTP. *Cell* **1995**, *81*, 891–904. [[CrossRef](#)]
183. Gao, Y.; Deng, K.; Hou, J.; Bryson, J.B.; Barco, A.; Nikulina, E.; Spencer, T.; Mellado, W.; Kandel, E.R.; Filbin, M.T. Activated CREB is sufficient to overcome inhibitors in myelin and promote spinal axon regeneration in vivo. *Neuron* **2004**, *44*, 609–621. [[CrossRef](#)] [[PubMed](#)]
184. Detke, M.J.; Johnson, J.; Lucki, I. Acute and chronic antidepressant drug treatment in the rat forced swimming test model of depression. *Exp. Clin. Psychopharmacol.* **1997**, *5*, 107–112. [[CrossRef](#)] [[PubMed](#)]

185. Hikida, T.; Jaaro-Peled, H.; Seshadri, S.; Oishi, K.; Hookway, C.; Kong, S.; Wu, D.; Xue, R.; Andrade, M.; Tankou, S.; et al. Dominant-negative DISC1 transgenic mice display schizophrenia-associated phenotypes detected by measures translatable to humans. *Proc. Natl. Acad. Sci. USA* **2007**, *104*, 14501–14506. [[CrossRef](#)] [[PubMed](#)]
186. Jin, S.L.; Richard, F.J.; Kuo, W.P.; D'Ercole, A.J.; Conti, M. Impaired growth and fertility of cAMP-specific phosphodiesterase PDE4D-deficient mice. *Proc. Natl. Acad. Sci. USA* **1999**, *96*, 11998–12003. [[CrossRef](#)] [[PubMed](#)]
187. Jin, S.L.; Conti, M. Induction of the cyclic nucleotide phosphodiesterase PDE4B is essential for LPS-activated TNF-alpha responses. *Proc. Natl. Acad. Sci. USA* **2002**, *99*, 7628–7633. [[CrossRef](#)]
188. Lee, H.; Graham, J.M., Jr.; Rimoin, D.L.; Lachman, R.S.; Krejci, P.; Tompson, S.W.; Nelson, S.F.; Krakow, D.; Cohn, D.H. Exome sequencing identifies PDE4D mutations in acrodysostosis. *Am. J. Hum. Genet.* **2012**, *90*, 746–751. [[CrossRef](#)]
189. Linglart, A.; Fryssira, H.; Hiort, O.; Holterhus, P.M.; Perez de, N.G.; Argente, J.; Heinrichs, C.; Kuechler, A.; Mantovani, G.; Leheup, B.; et al. PRKAR1A and PDE4D Mutations Cause Acrodysostosis but Two Distinct Syndromes with or without GPCR-Signaling Hormone Resistance. *J. Clin. Endocrinol. Metab.* **2012**, *97*, E2328–E2338. [[CrossRef](#)]
190. Michot, C.; Le, G.C.; Goldenberg, A.; Abhyankar, A.; Klein, C.; Kinning, E.; Guerrot, A.M.; Flahaut, P.; Duncombe, A.; Baujat, G.; et al. Exome sequencing identifies PDE4D mutations as another cause of acrodysostosis. *Am. J. Hum. Genet.* **2012**, *90*, 740–745. [[CrossRef](#)]
191. Lynch, D.C.; Dymont, D.A.; Huang, L.; Nikkel, S.M.; Lacombe, D.; Campeau, P.M.; Lee, B.; Bacino, C.A.; Michaud, J.L.; Bernier, F.P.; et al. Identification of novel mutations confirms PDE4D as a major gene causing acrodysostosis. *Hum. Mutat.* **2013**, *34*, 97–102. [[CrossRef](#)] [[PubMed](#)]
192. Lindstrand, A.; Grigelioniene, G.; Nilsson, D.; Pettersson, M.; Hofmeister, W.; Anderlid, B.M.; Kant, S.G.; Ruivenkamp, C.A.; Gustavsson, P.; Valta, H.; et al. Different mutations in PDE4D associated with developmental disorders with mirror phenotypes. *J. Med. Genet.* **2014**, *51*, 45–54. [[CrossRef](#)] [[PubMed](#)]
193. Brullo, C.; Ricciarelli, R.; Prickaerts, J.; Arancio, O.; Massa, M.; Rotolo, C.; Romussi, A.; Rebosio, C.; Marengo, B.; Pronzato, M.A.; et al. New insights into selective PDE4D inhibitors: 3-(Cyclopentylloxy)-4-methoxybenzaldehyde O-(2-(2,6-dimethylmorpholino)-2-oxoethyl) oxime (GEBR-7b) structural development and promising activities to restore memory impairment. *Eur. J. Med. Chem.* **2016**, *124*, 82–102. [[CrossRef](#)] [[PubMed](#)]
194. D'Ursi, P.; Guariento, S.; Trombetti, G.; Orro, A.; Cichero, E.; Milanesi, L.; Fossa, P.; Bruno, O. Further Insights in the Binding Mode of Selective Inhibitors to Human PDE4D Enzyme Combining Docking and Molecular Dynamics. *Mol. Inform.* **2016**, *35*, 369–381. [[CrossRef](#)] [[PubMed](#)]
195. Wu, Y.; Li, Z.; Huang, Y.Y.; Wu, D.; Luo, H.B. Novel Phosphodiesterase Inhibitors for Cognitive Improvement in Alzheimer's Disease. *J. Med. Chem.* **2018**. [[CrossRef](#)]
196. Robichaud, A.; Stamatiou, P.B.; Jin, S.L.; Lachance, N.; Macdonald, D.; Laliberte, F.; Liu, S.; Huang, Z.; Conti, M.; Chan, C.C. Deletion of phosphodiesterase 4D in mice shortens alpha(2)-adrenoceptor-mediated anesthesia, a behavioral correlate of emesis. *J. Clin. Invest.* **2002**, *110*, 1045–1052. [[CrossRef](#)]
197. Kreis, T.E. Microinjected antibodies against the cytoplasmic domain of vesicular stomatitis virus glycoprotein block its transport to the cell surface. *EMBO J.* **1986**, *5*, 931–941. [[CrossRef](#)]
198. Shepherd, M.; McSorley, T.; Olsen, A.E.; Johnston, L.A.; Thomson, N.C.; Baillie, G.S.; Houslay, M.D.; Bolger, G.B. Molecular cloning and subcellular distribution of the novel PDE4B4 cAMP-specific phosphodiesterase isoform. *Biochem. J.* **2003**, *370*, 429–438. [[CrossRef](#)]
199. Ye, Y.; Conti, M.; Houslay, M.D.; Farooqui, S.M.; Chen, M.; O'Donnell, J.M. Noradrenergic activity differentially regulates the expression of rolipram-sensitive, high-affinity cyclic AMP phosphodiesterase (PDE4) in rat brain. *J. Neurochem.* **1997**, *69*, 2397–2404. [[CrossRef](#)]
200. Shalin, S.C.; Hernandez, C.M.; Dougherty, M.K.; Morrison, D.K.; Sweatt, J.D. Kinase suppressor of Ras1 compartmentalizes hippocampal signal transduction and subserves synaptic plasticity and memory formation. *Neuron* **2006**, *50*, 765–779. [[CrossRef](#)]
201. Shalin, S.C.; Zirrgiebel, U.; Honsa, K.J.; Julien, J.P.; Miller, F.D.; Kaplan, D.R.; Sweatt, J.D. Neuronal MEK is important for normal fear conditioning in mice. *J. Neurosci. Res.* **2004**, *75*, 760–770. [[CrossRef](#)] [[PubMed](#)]
202. Paylor, R.; Crawley, J.N. Inbred strain differences in prepulse inhibition of the mouse startle response. *Psychopharmacology (Berl)* **1997**, *132*, 169–180. [[CrossRef](#)] [[PubMed](#)]

203. Rodgers, R.J.; Dalvi, A. Anxiety, defence and the elevated plus-maze. *Neurosci. Biobehav. Rev.* **1997**, *21*, 801–810. [[CrossRef](#)]
204. Kim, J.J.; Fanselow, M.S. Modality-specific retrograde amnesia of fear. *Science* **1992**, *256*, 675–677. [[CrossRef](#)] [[PubMed](#)]
205. Levenson, J.M.; O’Riordan, K.J.; Brown, K.D.; Trinh, M.A.; Molfese, D.L.; Sweatt, J.D. Regulation of histone acetylation during memory formation in the hippocampus. *J. Biol. Chem.* **2004**, *279*, 40545–40559. [[CrossRef](#)]
206. Moretti, P.; Levenson, J.M.; Battaglia, F.; Atkinson, R.; Teague, R.; Antalffy, B.; Armstrong, D.; Arancio, O.; Sweatt, J.D.; Zoghbi, H.Y. Learning and memory and synaptic plasticity are impaired in a mouse model of Rett syndrome. *J. Neurosci.* **2006**, *26*, 319–327. [[CrossRef](#)] [[PubMed](#)]
207. Miller, C.A.; Sweatt, J.D. Covalent modification of DNA regulates memory formation. *Neuron* **2007**, *53*, 857–869. [[CrossRef](#)]



© 2020 by the authors. Licensee MDPI, Basel, Switzerland. This article is an open access article distributed under the terms and conditions of the Creative Commons Attribution (CC BY) license (<http://creativecommons.org/licenses/by/4.0/>).